Journal of Structural Geology 32 (2010) 1590–1608

Contents lists available at ScienceDirect

Journal of Structural Geology

journal homepage: www.elsevier.com/locate/jsg

Evolution of cataclastic faulting in high-porosity sandstone, *Bassin du Sud-Est*, Provence, France

Elodie Saillet [a,*], Christopher A.J. Wibberley [b]

[a] *Geosciences Azur, UMR 6526, 250 Av. Albert Einstein, 06560 Valbonne, France*
[b] *TOTAL EP, CSTJF, Av. Larribau, 64018 Pau, France*

ARTICLE INFO

Article history:
Received 14 April 2009
Received in revised form
9 February 2010
Accepted 17 February 2010
Available online 6 March 2010

Keywords:
Reservoirs
Porous sandstones
Cataclastic Deformation Bands (CDBs)
"*Bassin du Sud-Est*"

ABSTRACT

Cataclastic deformation structures in Cretaceous high-porosity sands in the *Bassin du Sud-Est*, SE France were surveyed by scan-lines to examine: (i) the role of tectonic loading path on cataclastic deformation band (CDB) network development, and (ii) the development of larger ultracataclastic faults as strain increases. Deformation during Pyrenean–Provençal shortening resulted in a persistent high density ($\sim 10/m^2$) of conjugate reverse-sense CDB zones (displacements up to ~30 cm), with no generation of larger faults. High–low-density undulations occur for each pair of the conjugate set in an alternating manner, suggestive of network hardening, with a wavelength of several tens of metres being in the order of mechanical bed thickness. For two study areas which experienced significant Oligocene–Miocene extension, a moderate, undulating background density ($\sim 4/m^2$) of normal-offset CDBs was recorded, which became focussed in places into clusters ($\sim 50/m^2$) a few metres wide. Thus tectonic loading path may strongly influence strain distribution. CDB zones develop by the addition of successive bands at the edges until, at a thickness of around 5 cm, new bands tend to stray further away from the zone edges. Coarser sands have thicker CDB zones, suggesting that host grain size, along with mechanical bed thickness, could be an important contributor to the scale limit in CDB zone growth. Larger ultracataclastic faults and discrete slip zones localised within or at the edges of some clusters of CDB zones, post-date cluster development rather than inducing it. This stage of deformation evolution is only reached in extension, not in shortening, suggesting the infeasibility of achieving the critical state line during horizontal compression.

1. Introduction

Fluid circulation in the crust, and in particular hydrocarbon migration in reservoirs, is highly dependant on fault geometrical and hydromechanical properties (e.g. Manzocchi et al., 1998; Matthäi et al., 1998; Wibberley et al., 2008). Faulting in porous sandstone often produces zones of deformation bands rather than planar fracture surfaces (Aydin, 1978; Aydin and Johnson, 1978, 1983; Underhill and Woodcock, 1987; Antonellini et al., 1994; Davis, 1999; Fossen et al., 2007). Cataclastic deformation bands (CDBs) are brittle shear zones that form through a combination of compaction and cataclasis. Porosity and grain size reduction associated with CDB formation are thought to cause strain hardening, further deformation then being accommodated by deformation of the wall rock, adjacent to the initial band (Aydin, 1978; Aydin and Johnson, 1978, 1983; Underhill and Woodcock, 1987). Continued deformation may possibly result in the development of localised slip surfaces at the edge of deformation band zones (Aydin and Johnson, 1983; Antonelini and Aydin, 1995; Shipton and Cowie, 2001). Some, but not all of these different field observations have been understood through laboratory experiments (Wong et al., 1997; Mair et al., 2000; Torabi et al., 2007).

Descriptions of such deformation distributions in high-porosity sandstones are quite varied, ranging from examples of deformation band localisation as "damage zones" around larger faults, in relay zones (often expressed as "ladder zones" cf. Schultz and Balasko, 2003) or in fault-tip folds, to zones of deformation distributed over distances much greater than typical damage zone widths (e.g. ~100 m) with no obvious relationship to larger structures (Aydin, 1978; Underhill and Woodcock, 1987; Jamison and Stearns, 1982; Shipton and Cowie, 2001; Du Bernard et al., 2002a,b; Wibberley et al., 2007). Yet although recent advances have been made in understanding the mechanics of yielding to generate a single deformation band (e.g. Schultz and Siddharthan, 2005; Aydin et al., 2006; Wibberley et al., 2007), no unifying mechanical model exists for explaining and predicting distributions of deformation bands in

* Corresponding author. Tel.: +33 492942682.
E-mail address: saillet@geoazur.unice.fr (E. Saillet).

0191-8141/$ – see front matter © 2010 Elsevier Ltd. All rights reserved.
doi:10.1016/j.jsg.2010.02.007

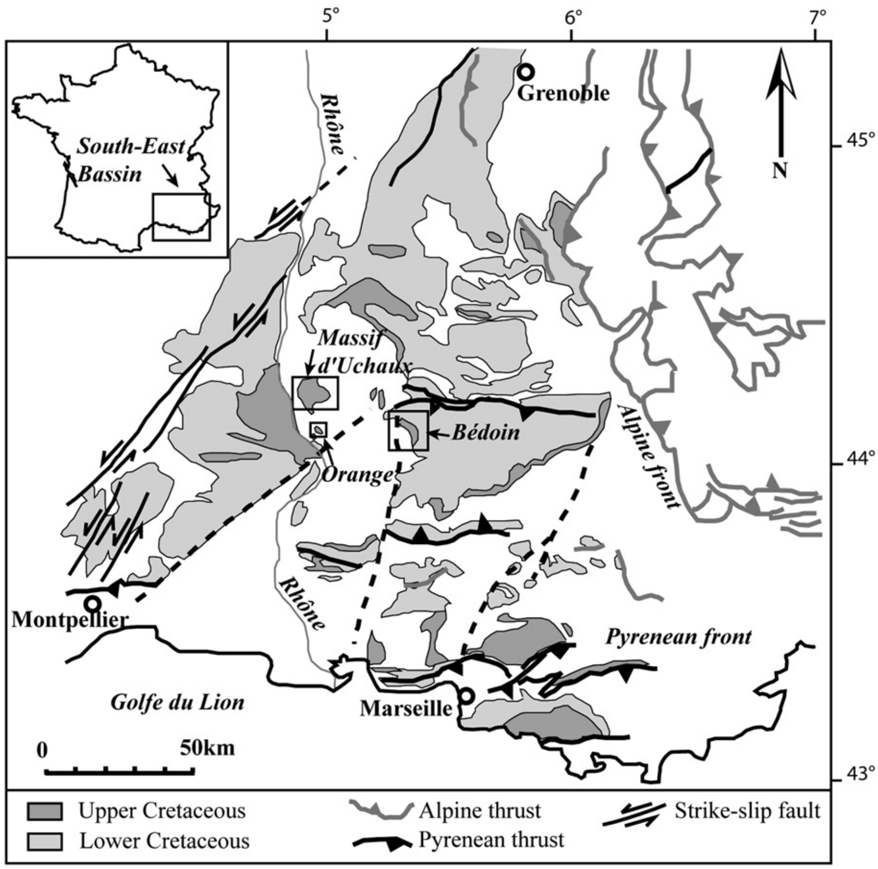

Fig. 1. Simplified geological and structural map of the study areas in the *Bassin du Sud-Est*, Provence, Southeast France. Locations of the three study areas are denoted by boxes. Modified from Wibberley et al. (2007).

terms of regional controls such as tectonic loading paths. Furthermore, the evolution of a network, and mechanical controls on this evolution, are still unclear, particularly with respect to localisation processes (a) at the scale of a single deformation band – what controls deformation localisation into a band, and deformation band growth? (b) at the scale of a cluster of deformation bands – do they become clustered around previously formed larger faults as fault "damage zones", or do the clusters of deformation bands form first, by early deformation localisation, with continued localisation of deformation generating the larger faults within or at the edges of these clusters? Some example of these behaviours exist (Fossen et al., 2000, 2007; Shipton and Cowie, 2001), yet understanding the mechanical controls on fault distribution is fundamental in order to provide better fault distribution prediction in reservoir flow simulations from limited structural input data (Saillet, 2009).

This paper presents a statistical and quantitative field study aimed at providing a model of deformation patterns and fault growth mechanisms in high-porosity sandstones. This study presents three different cases of Cretaceous high-porosity sands and sandstones in the *Bassin du Sud-Est*, Provence, France (Fig. 1). The field data were recorded along scan-lines from excellent quarry exposures from the Orange, Massif d'Uchaux and Bédoin areas (Fig. 1). These field data allow us to provide detailed descriptions of the distribution of deformation and its evolution, leading to interpretations in terms of fault growth mechanisms and fault network development in high-porosity sandstones. This part of the study concerns only the geometrical evolution of the deformation. The impact of deformed structures in sandstones on fluid flow, evaluated from permeability and geometric properties of the structures, will be addressed in a separate publication.

2. Geological setting and data acquisition

2.1. Regional context of the Bassin du Sud-Est

The *Bassin du Sud-Est* is a triangular region between the Massif Central to the North West, the Alps to the East, and the Mediterranean Sea to the South. It is a Mesozoic cratonic basin on the edge of the Alpine orogen, ~200 km long and 100–150 km wide. The total thickness of the sedimentary units is up to 10,000 m in the central area, but this thickness decreases to 2000–3000 m towards the edge of the basin (Delfaud and Dubois, 1984). From the Triassic to the Cretaceous, sedimentary deposits are essentially marine, corresponding to basin rifting related to Tethys opening. In the middle Cretaceous, the sedimentary units correspond to detrital sands deposited during the beginning of basin inversion. From late to end Cretaceous, the sands were deposited only in a continental environment, with locally high sedimentary rates (Debrand-Passard et al., 1984). In the West of the *Bassin du Sud-Est*, much of the resulting Cenomanian–Turonian deposits are high-porosity sands and poorly to moderately consolidated sandstones.

This paper presents a combined study of three areas in the *Bassin du Sud-Est*, the Bédoin, Massif d'Uchaux and Orange areas (Fig. 1). These studies were carried out on high-porosity sand and sandstone outcrops in active and abandoned quarries (Figs. 2–4), which provide excellent 2-D and 3-D exposures of deformation band networks and larger faults. These sands/sandstones are composed of a large range of quartz grain sizes which vary between the study areas. They also contain a few clay lamellae and, in places, limestone beds containing a few shallow marine fossils. These sands generally have a marine origin from deltaic to beach sands,

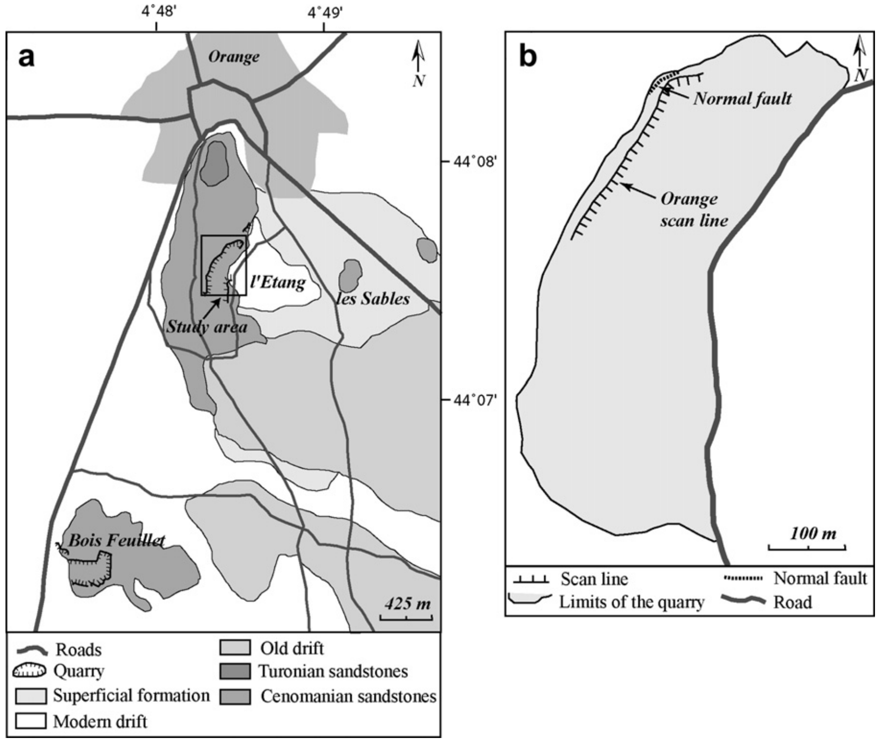

Fig. 2. (a) Location of the study area at Orange. Modified from the 1/50,000 geological map of Orange, BRGM. (b) Location of the scan-line within the sandstones from the "*Quartier de l'Étang*" quarry.

with some beds of aeolian origin. The sand outcrops show a low to moderate cohesion between the quartz grains due to a lack of cement, but can form vertical quarry faces for some months to years before erosion and outcrop collapse sets in. These sand units have undergone a low depth of burial, possibly less than 800 m (Delfaud and Dubois, 1984). Deformation is expressed in these sands and sandstone units as cataclastic deformation bands (CDBs), larger, ultracataclastic ("mature") faults and discrete slip surfaces (Wibberley et al., 2007). The orientation and kinematics of these structures are highly variable, but, from regional knowledge, can be attributed to the three different regional tectonic events in Provence: (i) North–South Pyrenean–Provençal shortening accommodated by regional foreland thrusting, giving the Cretaceous outcrop an East–West structural trend; (ii) NW–SE Oligocene–early Miocene rifting which caused normal faulting in parts of the Upper Cretaceous strata; (iii) Miocene left-lateral strike-slip reactivation of some of the major pre-existing NE–SW faults in the region.

2.2. Deformation features

The deformation features in the Cretaceous high-porosity sands and sandstones of the *Bassin du Sud-Est* consist of cataclastic deformation bands (CDBs) and larger ultracataclastic faults or discrete slip surfaces. At the outcrop scale the CDBs appear as single bands with millimetric offsets, usually grouped into zones of narrowly spaced bands with offsets from a few millimetres to tens of centimetres (Fig. 5). In most cases, the fine-scale sedimentary lamellae make it easy to determine apparent offsets. At the microscopic scale these CDBs are characterized by grain crushing and compaction (Wibberley et al., 2007). Such grain crushing and compaction resulted in a significant decrease in the porosity and permeability between the host sand and the deformed sand as previously described elsewhere (e.g. Underhill and Woodcock, 1987; Antonelini and Aydin, 1994; Fowles and Burley, 1994). The observations of these CDBs in the *Bassin du Sud-Est* suggest an evolution with displacement increase and thickness growth of the structures, similar to previous observations (Aydin and Johnson, 1978; Underhill and Woodcock, 1987; Antonelini and Aydin, 1995). The thinner features are deformation bands with very low displacements (e.g. <10 mm). These bands correspond to a single cataclastic fault strand with a thickness of one to a few millimetres. The SEM observations of these CDBs (Wibberley et al., 2007) show a preferential occurrence of fractures at grain contact points, suggesting a process of Hertzian fracturing (Gallagher et al., 1974). This observation also shows that, for a single CDB, this Hertzian fracturing process involves a zone typically not greater than five quartz grains wide. Scanning electron microscope (SEM) observations show that the processes of fracture and cataclasis produce a new generation of very fine grained fragments infilling the porosity space.

Thicker features are "multiple strand" zones of cataclastic deformation bands (e.g. 10–300 mm in displacement, 10–100 mm wide) formed by generation of successive adjacent single bands, referred to hereafter as "CDB zones". The adjacent bands within these CDB zones can be generated with a variable spacing. At the outcrop scale it is not easy to distinguish the different bands within a CDB zone, except where there are lenses of host sand between the different bands. Field observations show that the number of individual bands in a CDB zone correlates with offset, up to the scale limit of the deformation bands, around 30 cm offset (Wibberley et al., 2000). This finding contrasts with studies of the number of discrete slip surfaces in fault core zones in high-porosity sandstones which show no correlation with offset (Shipton et al., 2005).

Larger faults, with offsets greater than around 1 m, are also present in the high-porosity sands and sandstones of the *Bassin du Sud-Est*. These faults appear to have been generated separately from the smaller-offset CDBs, in some cases during a later tectonic event

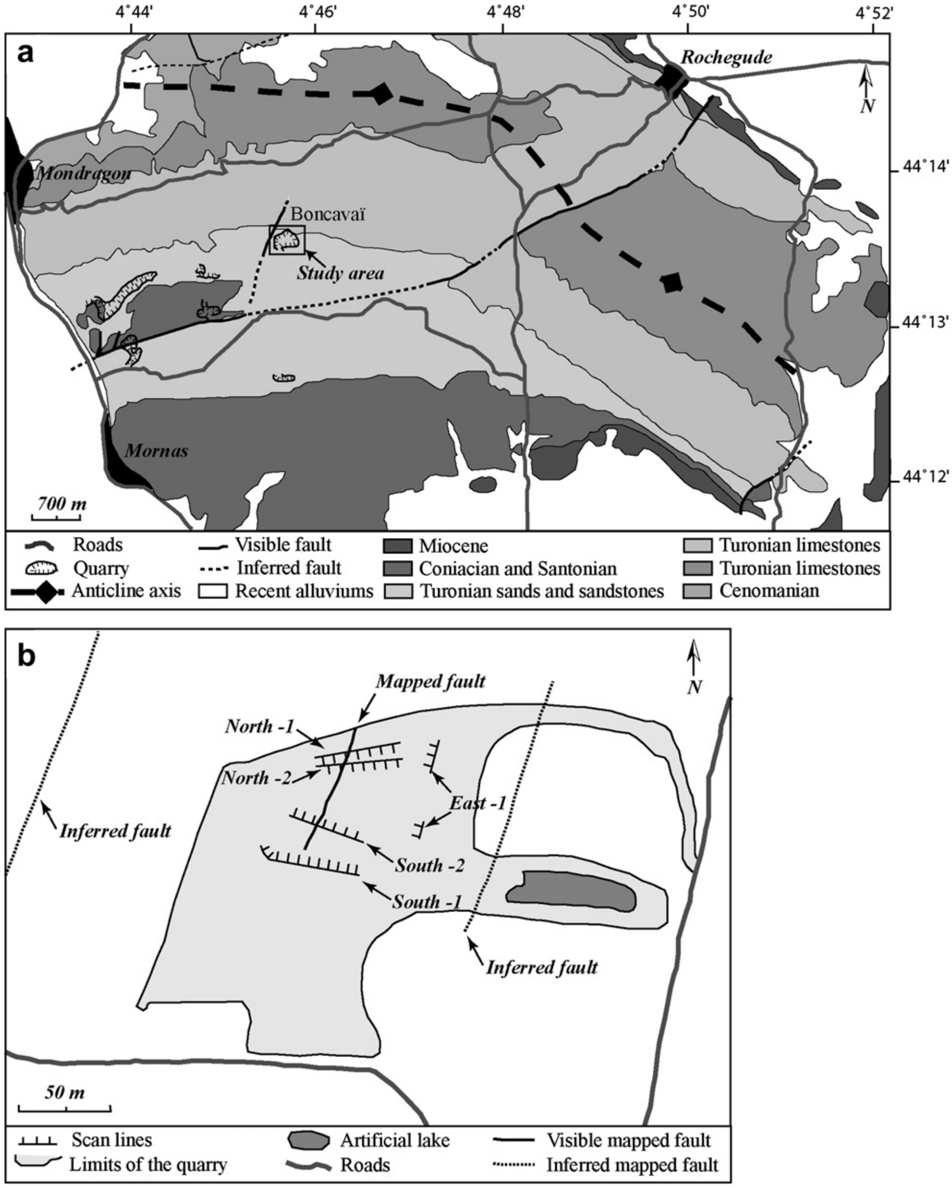

Fig. 3. (a) Location of the study area in the Massif d'Uchaux. Modified from the 1/50,000 geological map of Orange, BRGM. (b) Location of the different scan-lines within the "*Boncavaï*" quarry.

than those forming the cataclastic deformation bands. These larger faults present drastic differences in their properties and characteristics compared to the CDBs. On the field scale, these faults show a fairly homogeneous deformation zone of ultracataclastic fault rock, with sometimes one or more discrete slip surfaces in the fault core, and a cluster of anastomosing cataclastic strands around the edges of the fault zone (Fig. 6). At the microscopic scale there are also large differences between these faults and the CBD microtextures. SEM photomicrographs (Wibberley et al., 2007) show some rounded quartz grains of original sedimentary size and a higher proportion of ultrafine material than in CDBs. These differences seem to reflect a transition in fault growth mechanisms from CDBs to larger faults, yet there are a relatively small number of these ultracataclastic fault zones in the study areas. In the Orange and Bédoin areas, these mature faults are normal faults, post-dating the earlier reverse-sense CDBs. In the Massif d'Uchaux area they are large strike-slip faults, cross-cutting the earlier normal-sense CDBs. Thus, in some cases at least, deformation localisation into ultracataclastic fault zones is encouraged by the presence of an earlier set of deformation bands of high density (Wibberley et al., 2007).

2.3. Field data acquisition

In order to characterise the deformation distribution in each area, the CDBs were sampled by scan-lines made on each outcrop. The position of all visible CDBs or larger faults was recorded along one metre-wide scan-lines (thus structural density, rather than frequency, is recorded), perpendicular to the strikes of the main structures. This methodology is similar to at least some of the previous studies of this type elsewhere (e.g. Du Bernard et al., 2002b). Because of our rectilinear quarry topography, it is not necessary to make any statistical correction in the CDB positions on the outcrop, although density corrections were performed for dip obliquity between (horizontal) scan-line and non-vertical structures (Priest and Hudson, 1981). For each CDB, the orientation, the

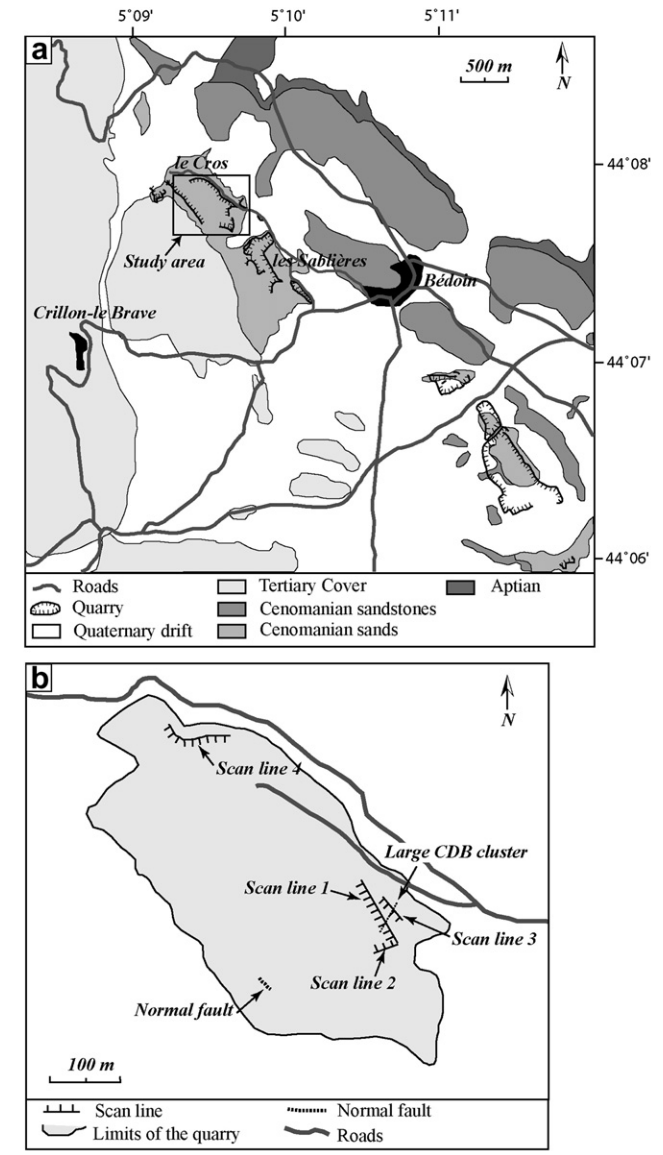

Fig. 4. (a) Location of the study area in the region of Bédoin. Modified from the 1/50,000 geological map of Vaison la Romaine, BRGM. (b) Location of the different scan-lines within the sands from the "*Le Cros*" quarry.

thickness, and the number of CBDs in a CDB zone and their offset were recorded in order to statistically analyse each outcrop. CDB zones are grouped into a single structure provided that the outermost strands are no further from the remaining structure than the thickness of the remaining structure, and that they converge to touch the structure. A total scan-line length of 717 m was recorded for the 3 study areas combined.

3. The distribution of deformation

3.1. Outcrop description

3.1.1. Orange sandstones

The Orange study area is located in the abandoned *Quartier de l'Etang* quarry, on the south side of the town (Fig. 2). The outcrop is composed of different sedimentary units of Cenomanian age. The majority of the quarry is composed of a cohesive (not disintegrating to the touch) quartz sandstone unit, mineralogically mature, but texturally immature, with a high porosity partly due to the small proportion of quartz cement. This sandstone unit has a marine to beach origin, and is composed of medium-size quartz grains of average size of 550 μm. At outcrop, it is possible to observe some sedimentary channel structures formed in a marine environment, and in other parts of the outcrop some benthic shallow marine fossils are present. The sandstone unit is covered by a calcarenite unit, the contact between these two units dipping around 8° to the South-West. The deformation of the sandstone unit of the *Quartier de l'Etang* quarry consists of conjugate reverse-sense CBDs with a low angle of dip (34° to 37°) and an ESE–WNW trend thought to be related to N–S Pyrenean–Provençal shortening (Figs. 5, 7a). At the Orange outcrop, there are also a small number of high-dip (around 80°) normal CDBs which were formed during a later tectonic event (Fig. 7a). A mature, larger normal fault (10 m displacement) is also present. One single scan-line 258 m long has been recorded from the Orange study area.

3.1.2. Massif d'Uchaux sands

The Massif d'Uchaux study focuses on the excellent exposure provided in the *Boncavai* quarry, to the northeast of the town of Mornas. The study area is made up of different Turonian (late Cretaceous) sands and sandstones. All the outcrops studied are situated within the same sand units. These sand units have a very low cohesion (crumble to the touch) and are essentially composed of moderate to large quartz grains, with a few clay lamellae. These incohesive sands are organized in centimetre-scale fining-upwards units. These observations suggest sand deposition in an inter-tidal deltaic environment. The *Boncavai* quarry area is situated on the south side of an anticline structure of WNW–ESE trend (Fig. 3). At the scale of the quarry, the deposits have a constant dip of a few degrees to the Southeast. The deformation of the Turonian sands is essentially expressed as normal-sense conjugate CDBs trending NNE–SSW corresponding to ESE–WNW Oligocene extension (Fig. 7b). There is widespread evidence that these CDBs act as barriers to recent and present-day groundwater flow, because of the haematite-coloured grain-coating deposits in the sand adjacent to the faults. This coloration marking the local limits of fluid percolation down through the sand in the vadose zone and/or Liesegang ring type diffusion, although the mechanism of fluid-rock interaction responsible for this is currently not clear and is the subject of parallel research. A few low-angle reverse CDBs were cut by the normal structures, probably corresponding to the Pyrenean–Provençal shortening (Fig. 7b). A mature strike-slip fault is also present cross-cutting the normal CDBs, probably related to the regional Miocene strike-slip faulting (Fig. 7b). Data from this study area were collected from five different rectilinear scan-lines along the outcrops, with a total length of 209 m.

3.1.3. Bédoin sands

The Bédoin study area centres on the *Le Cros* quarry which is still periodically active, to the North West of the village of Bédoin, South of Mt. Ventoux (Fig. 4). The *Le Cros* quarry is composed of a single sand unit several tens of metres thick, with a low cohesion (crumble to the touch), of Cenomanian age. The *Le Cros* quarry sands have very fine to intermediate quartz grain size and a few clay lamellae. The deposition of this unit probably occurred in a beach to marine environment, with occasional evidence for transition to an aeolian-type deposition. This unit has a constant low dip (a few degrees) to the South-West. As in the Massif d'Uchaux area, the CDBs of Bédoin exert an influence on present-day groundwater flow, as evidenced by the haematite-red deposits of grain-coatings adjacent to some of the CDB clusters. The sands of the Bédoin area show deformation structures generated during three different tectonic events. A set of reverse, conjugate low-angle CDBs

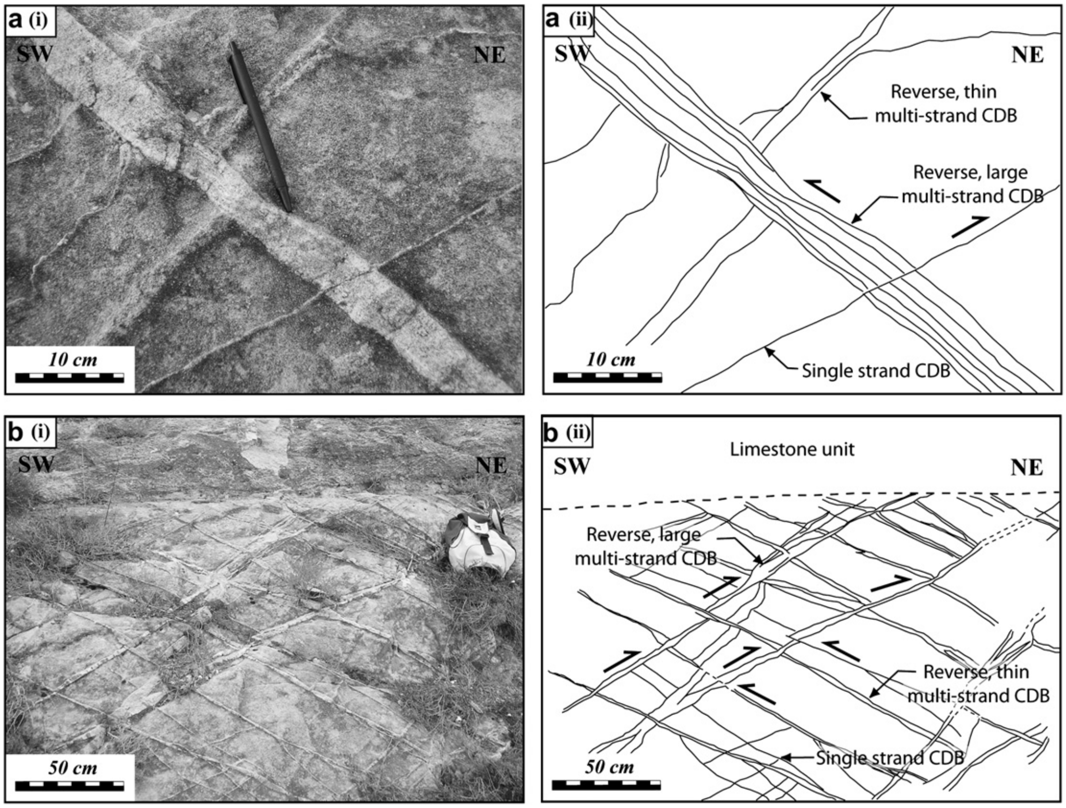

Fig. 5. Field appearance of conjugate arrays of cataclastic deformation bands in the Upper Cretaceous sandstones at the Quartier de l'Etang quarry, Orange. a) Detailed field view of the alternating chronology between structures of two conjugate sets. (i) Field photo; (ii) interpretative field sketch. b) Broader field view of the generally synchronous, but locally alternating, relationships between two conjugate sets of reverse CDBs and CDB zones. (i) Field photo; (ii) interpretative field sketch.

is present, with a broadly E–W to NE–SW trend, formed during N–S Pyrenean–Provençal shortening. This first fault generation is cross-cut by a large population of steeply dipping normal, conjugate CDBs trending WSW–ENE probably corresponding to Oligocene–Miocene extension (Fig. 7c). This second tectonic event is also responsible for the presence of a larger, mature normal fault zone with a localised slip plane and a throw on the order of 10 m. Subvertical CDBs with a NW–SE trend (Fig. 7c) post-date the other structures and are interpreted as having formed during later strike-slip faulting during the Miocene. Data were collected from four different rectilinear scan-lines along the outcrops, with a total length of 250 m.

3.2. Description of CDB densities

In this sub-section, data on the distribution of CDBs and larger faults from the outcrops for the three study areas are presented, in order to investigate the controls on the density of developing arrays of deformation bands and faults. For each outcrop the CDB density is defined as the number of CDBs per square metre plotted as a function of distance along the scan-line.

3.2.1. Orange sandstones

The deformation recorded in the Orange study area corresponds mostly to one single tectonic event, expressed as low-angle conjugate reverse faulting. A later extensional event generated only a small number of normal CDBs and larger "mature" ultracataclastic faults. Data corresponding to these reverse CDBs were obtained along one single scan-line 258 m long. Because of the angle of 40° between orientation-dip of the structures and the scan-line, it is important to make a correction to the field-measured density values (D_{field}). The angle correction (D_{corr}) is obtained (Priest and Hudson, 1981) by using the equation (1):

$$D_{corr} = D_{field} \times 1/[\sin 35^\circ] \qquad (1)$$

On the density profiles, the D_{corr} and the D_{field} are given. The density profiles obtained illustrate three important features (Fig. 8):

1. The CDB density scan-line corresponding to the total data set of the conjugate reverse fault population shows a persistently high density (generally in the range 7–15/m^2), and a more-or-less continuous distribution of the deformation along the outcrop, with a clustering in the South (Fig. 8a). The clusters of CDBs on the South side of the outcrop correspond to the presence of ladder zones of very thin CDBs and do not impact significantly on the overall distribution of strain.
2. The CDB density variations corresponding to the two different (opposing dips) sets of the conjugate fault population show a more heterogeneous distribution of deformation (Fig. 8b, c). The density profile corresponding to the SW-dipping conjugate population shows a high CDB concentration in the south, middle and north of the outcrop but low-density "voids" around 100 and 160 m (Fig. 8b). The density profile corresponding to the opposite set (North-dipping) of the conjugate population shows a high CDB concentration around 100 and 160 m but important "voids" in the South, in the centre at around 120 m, and in the North (Fig. 8c). As illustrated by the vertical dashed arrows in Fig. 8b and c, these "voids" or troughs in the NE-dipping set density profile coincide closely with the

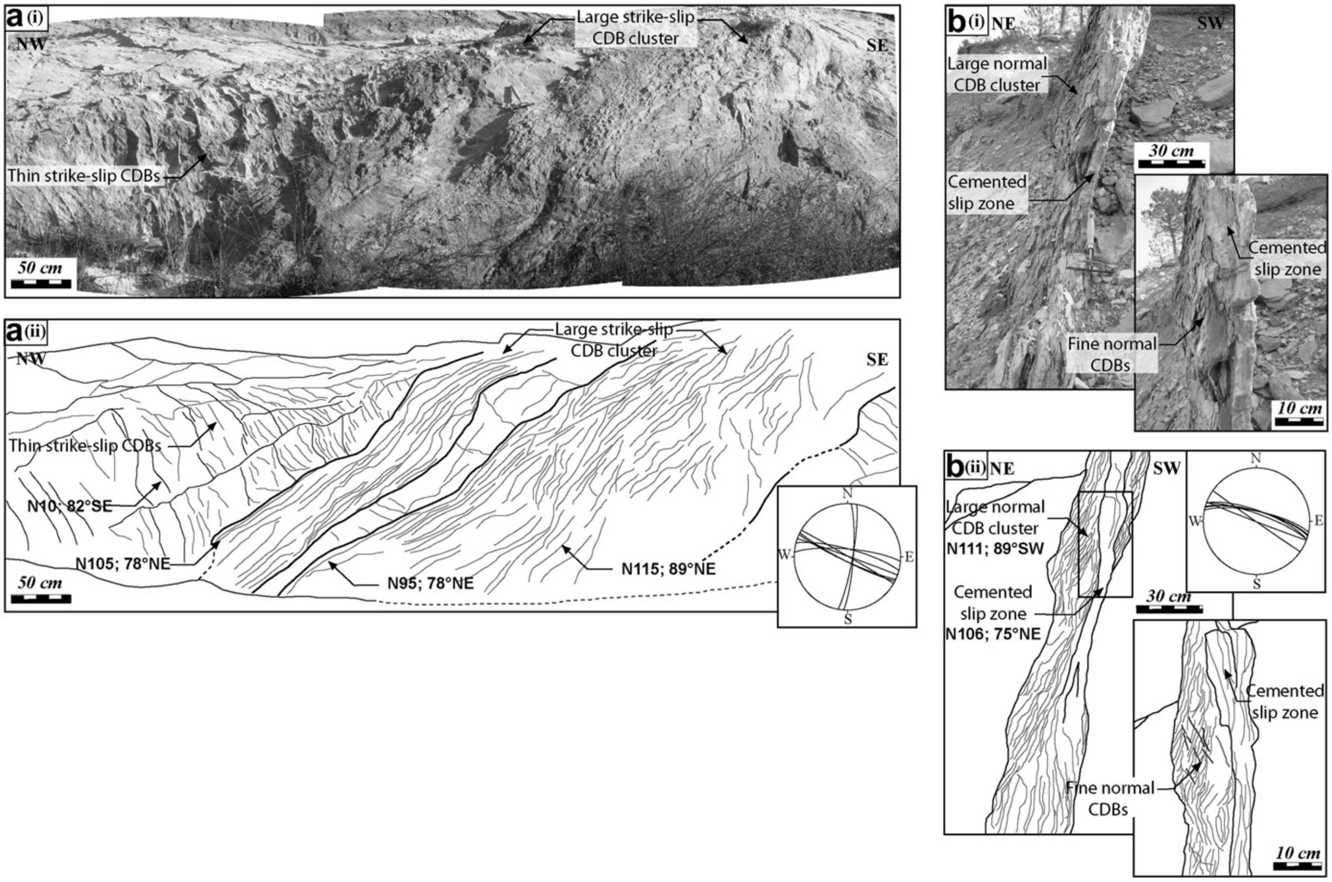

Fig. 6. Field appearance of relationships between thin CDBs, large clusters and a slip zone in the Upper Cretaceous sands of the Le Cros quarry at Bédoin. a) Field view of the relationships between earlier thin structures and two larger CDB clusters with strike-slip kinematics. (i) Field photo; (ii) interpretative field sketch. b) Field view of the relationships between a cemented slip zone within a large CDB cluster of normal fault kinematics. The field observations show that earlier CDBs cluster is cut by the slip zone. (i) Field photo; (ii) interpretative field sketch.

positions of high-density zones of the SW-dipping set, and vice versa, i.e. that there is a spatial correlation between the high density of one of the conjugate sets and a low density of the other. A statistical analysis of deformation distribution, based on the clustering tendency as used in Wibberley et al. (2007), improved to analyse a range of data bin sizes, shows that each of the two conjugate sets is much more clustered than the overall population treated as a single ensemble (Fig. 9). Furthermore, the cluster analysis is strongest for bin sizes in the order of ~60 m along the scan-line (Fig. 9), converting to a wavelength of around 30 m when the dip correction is applied to these low-angle structures, i.e. on the order of bed thickness.

3. The larger normal fault, on the North side of the outcrop (Fig. 2), corresponding to a later tectonic event, has no spatial correlation with any of the reverse structures. It has a throw of ~10 m and is an ultracataclastic fault zone around 75 cm wide where measured. The microstructures show an intense decrease of grains and pores size, which can significantly retard fluid flow (Saillet, 2009). Additionally, Wibberley et al. (2007) show that larger faults form preferentially in regions which have already recorded an earlier deformation event.

3.2.2. Massif d'Uchaux sands

The deformation of the Massif d'Uchaux is essentially expressed by a population of normal-sense conjugate CDBs and later strike-slip faults. A low number of small low-angle reverse-sense CDBs are present, probably generated by an earlier tectonic event. The density profiles (Fig. 10) corresponding to the different outcrops show essentially the conjugate and normal CDBs but some strike-slip faults are also present including a large “mature” ultracataclastic strike-slip fault which crosses the entire quarry outcrop (Fig. 3). On each profile the position of this large strike-slip fault is indicated. The density profiles (Fig. 10) illustrate three important features:

1. The different density profiles show similar patterns of spatial deformation distribution. The most striking feature of this pattern is the relatively persistent, in relation to precedent publications (Du Bernard et al., 2002b), yet undulating background distribution of the deformation over the length of the 45–60 m scan-lines.
2. For all the outcrops there are a few zones which present an anomalous CDB density increase in addition to the moderate overall density (Fig. 10). These zones of high-density concentration are ladder zone features such as in the middle of the outcrop “South-1”. The anomalous weighting effect of small ladder zones on density profiles has been checked by also plotting profiles of cumulative thickness per square metre (not presented in this paper for simplicity). In such a case the outcrop shows a more even deformation distribution because each ladder zone is a high density of very thin features, impacting much less on cumulative thickness profiles. In other

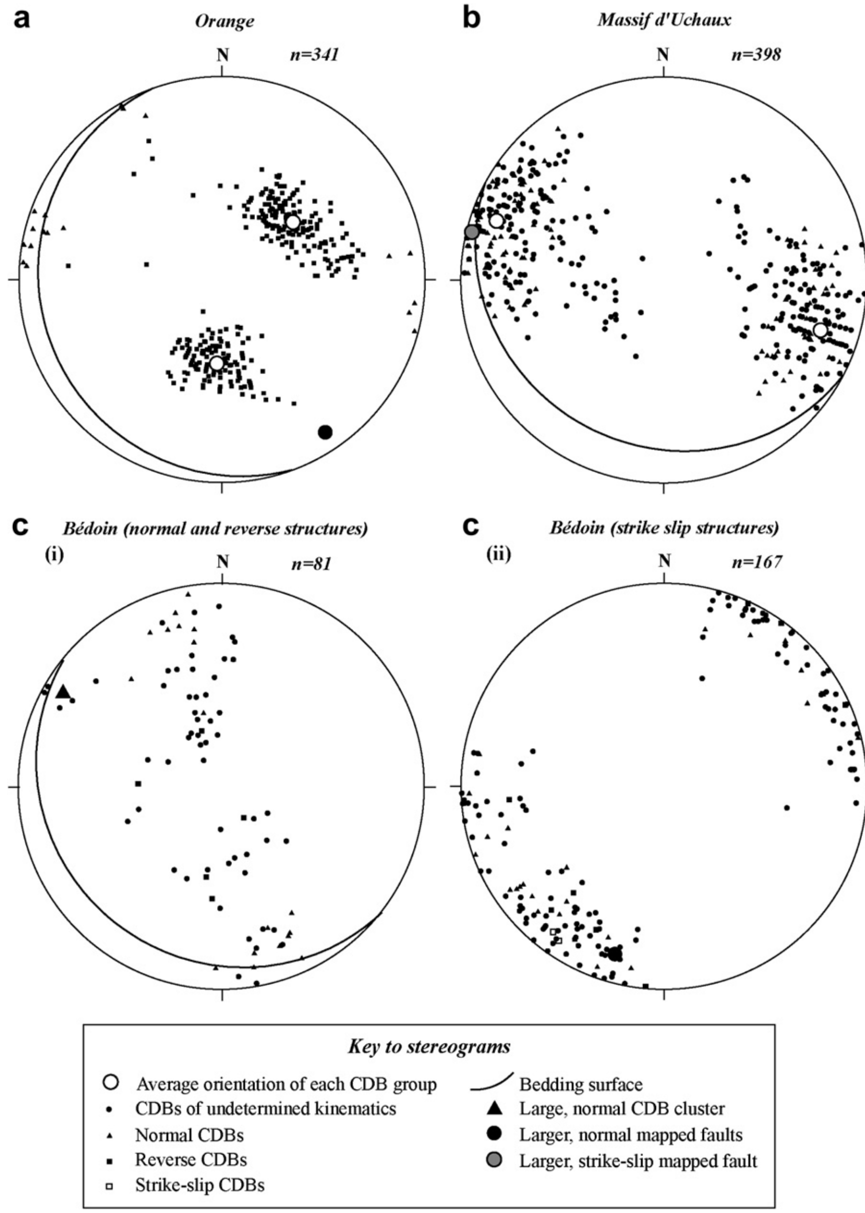

Fig. 7. Lower-hemisphere equal-area stereographic projections (stereograms) of poles to planes for cataclastic deformation bands and larger faults from the studied areas. (a) Data from the Orange area; (b) data from the Massif d'Uchaux area; (c) data from the Bédoin area.

parts of the outcrop there are increases of CDB density unrelated to specific structures such as a larger fault.

3. All the outcrops studied are cut by the same large ultracataclastic strike-slip fault zone (with bedding-parallel striations) which is systematically correlated with a large CDB density increase. Nevertheless, it is difficult to determine the kinematics of these CDBs which are present around the larger fault and hence infer the tectonic event which generated them. The CDBs clustered around the main strike-slip fault zone show normal apparent offset in the vertical outcrop views, but due to the geometry of the dip of the CDBs and the dip of the stratigraphy they may in reality be normal or strike-slip structures. Hence the relative timing of background CDBs with respect to clusters is not inferred by these observations.

All the Massif d'Uchaux scan-lines show relatively similar deformation distribution patterns and CDB densities. These density distribution diagrams illustrate three important features: (i) The overall CDB density is moderate (mean values are given in Fig. 10), with the predominance of single CDBs and thin CDB zones; (ii) A few patches present anomalous CDB density increases, where CDB zones are organized in clusters; (iii) These clusters are not systematically associated with main slip surfaces or larger ultracataclastic fault zones, but those slip surfaces or fault zones that are present do exist within or at the edges of clusters of CDB zones.

3.2.3. *Bédoin sands*

Three different events have been recorded by the outcrops of Bédoin and are evidenced along each of the four scan-lines recorded in the study area (Fig. 4): the Pyrenean–Provençal shortening, the Oligocene–Miocene extension and the strike-slip faulting during the Miocene. However, offset along the CDBs and CDB zones is of a similar magnitude to the CDB zone thickness, and displacement is only visible to the naked eye for the larger features. Hence it

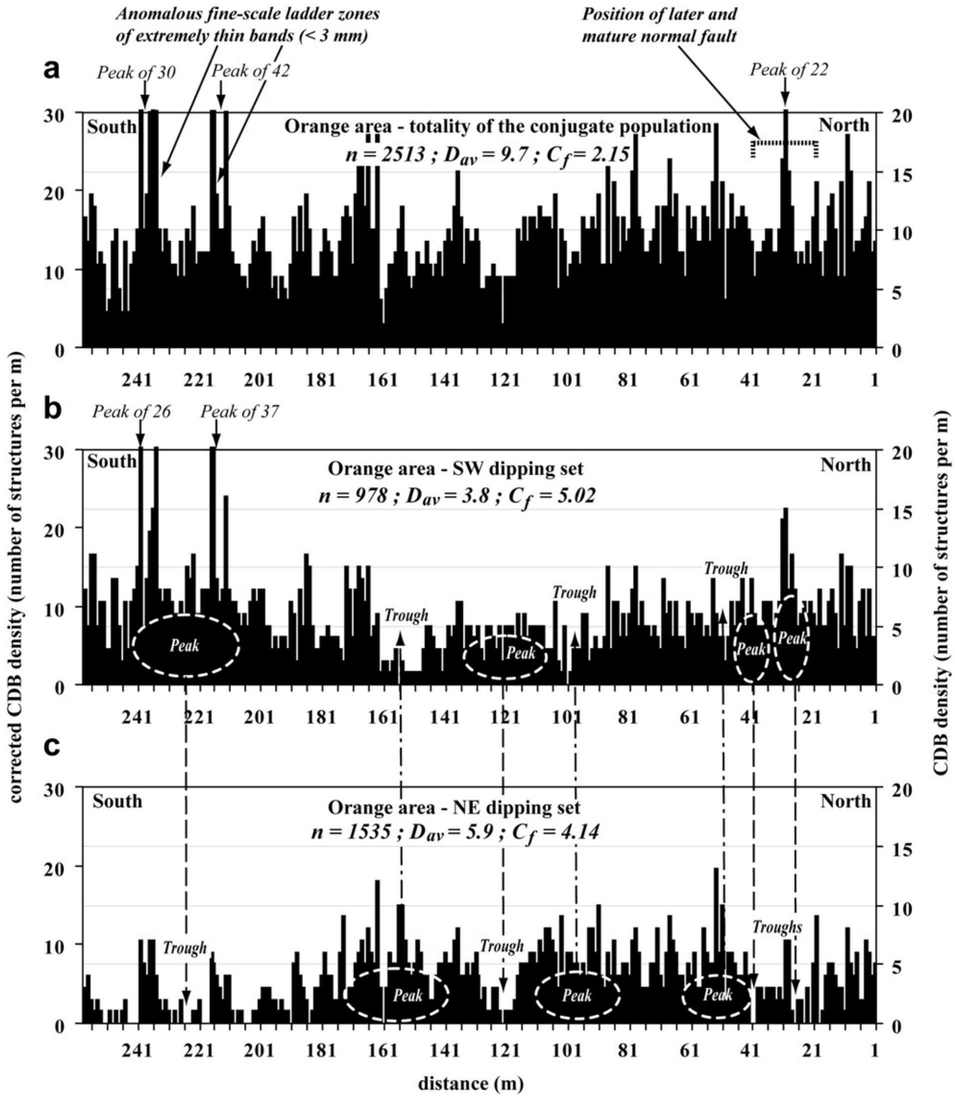

Fig. 8. Graphs of CDB densities for the conjugate, reverse structures recorded along the 258 m long outcrop of the "*Quartier de l'Etang*" quarry in the Orange area. Density is defined as the number of CDBs per square metre, directly measured on the field or with angle correction (see text for more details). (a) The overall sum of the CDBs present in the scan-line of the outcrop. (b) Density distribution of the SW-dipping CDB set. (c) Density distribution of the N-dipping CDB set. For each graph *n* is the total number of deformed structures and D_{av} is the mean average density directly measured on the field (without angle correction). Cf is the cluster factor in each case (see text for details).

is very often not possible to determine the kinematics of any one CDB structure. The density profiles obtained on the scan-lines (totalling 250 m in length) illustrate three important features similar to those of the Massif d'Uchaux area (Fig. 11):

1. There is generally an overall deformation pattern of undulating moderate CDB density which constitutes a "background" deformation along the outcrops.
2. All the different outcrops from the Bédoin study area show some patches with an increase in the density of structures corresponding to a localisation of the deformation within a few clusters of CDB zones. These clusters are 5–10 m wide with a CDB density comprised between 30 and 50 structures per square metre, for a general density average comprised between 6 and 10 structures. These clusters do not generally coincide with the position of any larger fault, except in one case (scan-line 3, Fig. 11).
3. Although there are not many larger faults visible at the outcrops in the Bédoin study area, it is possible to identify two larger structures. The first one is situated on scan-line number 3 (Figs. 4 and 11), where it is possible to observe a progressive increase of the CDB density to a maximum in the centre of the cluster, beyond which the density drops sharply to define the other edge of the cluster. Localisation of a discrete slip surface occurred at this sharp transition region at the edge of the cluster. On this first structure it is difficult to determine the relative timing of cluster and slip surface because of the poor condition of the outcrop. The second structure is situated on the south side of the quarry and was not sampled by any scan-line because of the orientation of the fault with respect to the outcrop. Nevertheless, it is also possible in this case to observe a cluster of CDB zones around a central slip surface with the same orientation and dip. Given that many clusters exist with no localised slip planes or larger fault zones, it seems logical to suggest that the clusters evolved first, only some of which then localised deformation into more evolved fault and/or slip zones.

The Bédoin scan-lines show relatively similar deformation distribution patterns to the Massif d'Uchaux outcrops: (i) The overall CDB density is undulating but generally moderate, with

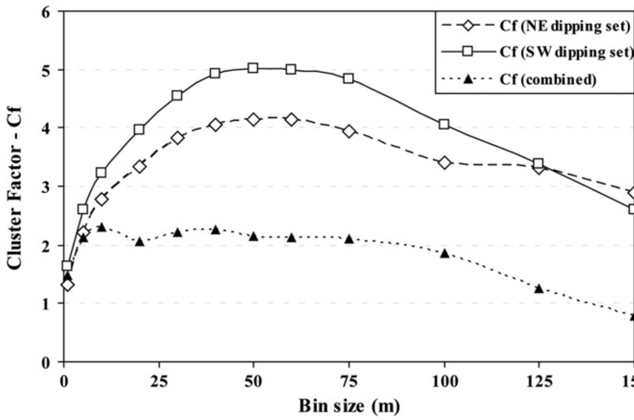

Fig. 9. Graphs of cluster factor versus bin size using the definition of Wibberley et al. (2007) adapted for analysing the size of the "most likely" periodic clustering by repeating the cluster factor analysis for a range of different bin sizes, displacing the bin along the scan-line at 1 m intervals. Results are theoretically independent of sample size, hence the result that each conjugate set has a cluster factor twice as high as the ensemble of the conjugate fault population (peaking at around 50–60 m bin size) suggests that the more even distribution of CDBs in the overall population is the result of summing the more clustered distribution of peaks and troughs of the two conjugate sets together.

mean scan-line averages between 6 and 10 structures per m; (ii) A few zones of anomalously high CDB density exist (with density of 30–50 structures per m), where CDB zones are organized into clusters; (iii) These clusters are not systematically associated with discrete slip surfaces or ultracataclastic fault zones, but ultra-cataclastic fault zones are sometimes present within the maximum density of CDB zones. In the Bédoin area the deformation features correspond to three different tectonic events and in some cases it is not possible to determine the kinematics or displacement with the naked eye.

4. Characterisation of individual CDB properties based on field data

4.1. Fault thickness data

Previous studies of the relationship between fault zone thickness and fault displacement (Robertson, 1983; Scholz, 1987; Hull, 1988; Evans, 1990) have generally shown that although there is an overall linear relationship between fault zone thickness and displacement, it is necessary to take account of various problems like the definition of the edges of the fault zone or the thickness variation along a single fault when interpreting data. Fault zone thickness–displacement data are presented in Fig. 12, for single CDBs, CDB zones and larger ultracataclastic fault zones in the study area of the sandstones from Orange and the incohesive sands from Massif d'Uchaux and Bédoin. The data are presented with two different thickness data measurements. Thicknesses using method 1 are given as the total distance between the outermost edges of the outermost strands constituting the multiple-band CDB zones. With this first measurement method the host sand contained in between the different strands of a multiple-band CDB zone is included in the measurement. Thicknesses using method 2 are given as the sum of the thicknesses of each individual band constituting a multiple-band CDB zone. This second measurement method defines an "effective thickness" of deformed material, taking into account that material between the bands is undeformed host sand.

There are sufficient similarities between the data from the three study areas to be able to generalize the observations in the following way:

1. Fault (or CBD) thickness is often equal to (with a thickness–displacement ratio approximately equal to 1) or smaller than displacement (with a thickness–displacement ratio between 1 and 0.1), with a general linear relationship despite this variation.
2. For the larger structures ($d > \sim 100$–500 mm), a proportional increase between thickness and displacement does not clearly exist.
3. Where thickness data were also collected using method 2 or "effective" thickness data, these thicknesses recalculated as the sum of the individual strands show a steady general decrease in ratio of "effective" thickness of deformed material to displacement as displacement increases. In other words, as displacement increases, additional increments of displacement result in decreasing amounts of added volume of deformed material.
4. Larger normal faults (throw > 1 m) and CDBs/CDB zones are plotted on the same graph for comparison. These faults fall in a different class of structures and they show different microstructure and deformation mechanisms. These ultracataclastic fault zones have much lower thickness–displacement ratios than CDBs and CDB zones.
5. Where clay layers are intersected, the structures have thickness–displacement ratios at the lower end of the range of data.
6. Where structures were formed in different tectonic events at the same outcrop, no significant differences are detectable between data corresponding to the different events.

4.2. Fault thickness distribution data

Fig. 13 shows the fault thickness distribution data for all of the outcrops studied in the *Bassin du Sud-Est*. For each different study area, all of the structures recorded along the scan-lines are presented. Data are not divided into kinematic groups, because kinematics was not discernable in many cases, and so leaving such data out would generate artificial trends, particularly in the exclusion of the single CDBs and thinner CDB zones for which offsets were most difficult to discern with the naked eye. The three different study areas exhibit the same general pattern, that there is a predominance of thin CDB zones of small displacement. For example, only 20% of the structures have thickness greater than around 1 cm (0.6–2 cm depending on the study area). There is a much lower proportion of larger (wider) CDB zones and ultracataclastic fault zones than small CDB zones. Differences in the fault thickness distribution data between the three study areas relates closely to the initial host sand grain size: the larger host sand grain size has thicker structures, and the lower host sand grain size has thinner ones (Fig. 13).

4.3. CDB, cluster and fault zone internal structure

Fig. 14 presents information on the internal structure of CDB zones in terms of the number of individual cataclastic bands identifiable to the naked eye within a CDB zone in relation to its thickness. These data are presented separately for the three different study areas. The data corresponding to the Orange area have been recorded only using thickness measurement method 1 (Fig. 14a), i.e. the overall width of the CDB zone from one edge to the other. Method 2 was not used because it was not possible to precisely distinguish the limits of the zones of cemented host grains from the white strands of the deformation band structure with the naked eye. It was, however, possible to detect strands as "whiter" zones and tentatively count them. Data from the Massif d'Uchaux and Bédoin areas have been presented using both method 1

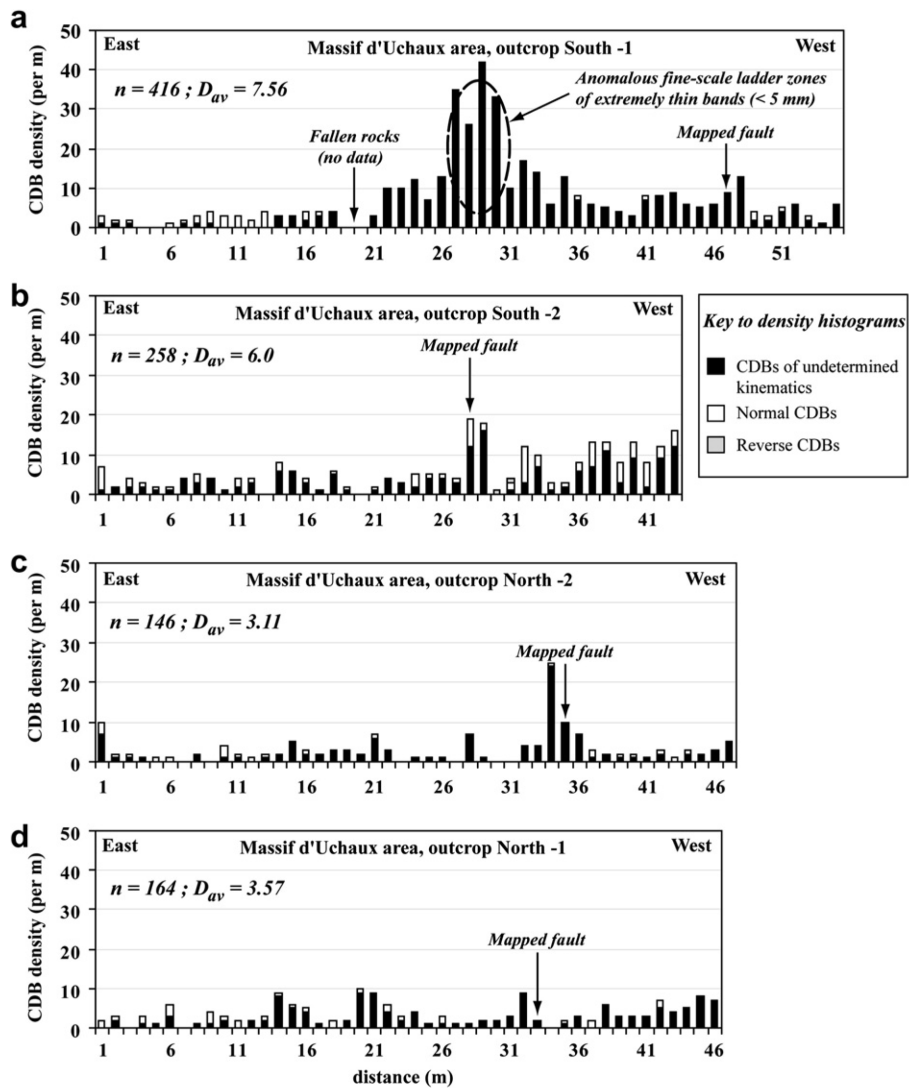

Fig. 10. Graphs of CDB densities for the normal and strike-slip structures recorded along scan-lines with a total length of 209 m in the "*Boncavai*" quarry in the Massif d'Uchaux area. Density is defined as the number of CDBs per square metre. The CDB density overall is moderate, with localisation of deformation within clusters of deformation bands. For each outcrop, n is the total number of deformed structures and D_{av} is the mean average density.

(Fig. 14b(i) and c(i)) and method 2 (Fig. 14b(ii) and c(ii)) thickness measurements. Thicknesses using method 2 are given as the sum of the thicknesses of each of the individual bands constituting a multiple-band CDB zone or individual high-strain zones in an ultracataclastic fault zone.

The data on the cataclastic bands in the CDB zones corresponding to the three different study areas show the same overall patterns of increase in the number of strands with increase in thickness. In general, the CDB zones show a linear dependence of the number of bands with increase in thickness, suggesting that CDB zones develop by formation of additional bands successively at the edges of the structure as deformation continues. Multiple-band CDB zones with identifiable undeformed sand in between the bands are typically recorded as thicker structures for a given displacement than those CDB zones with no host sand within the structure (Fig. 14b(i), c(i)) but when the effective thickness of fault rock (thickness method 2) is plotted, it seems clearer that the thickness of fault rock increases as a function of displacement in the same way for the two types of structures: the best-fit relation for the effective thickness for both types of structure together (Fig. 14b (ii), c(ii)), being very close to the best-fit relation of overall thickness (method 1) for the CDB zones with no host sand within them. For the data from Bédoin (Fig. 14c), the CDB zones thicker than around four centimetres a different trend is apparent: a disproportionate thickness increase with addition of new bands (Fig. 14b(i), c(i)) collapses onto a single linear trend when the data are re-plotted in terms of effective thickness of deformed fault rock (Fig. 14b(ii), c(ii)). This indicates that CDB zones growing wider than around 50 mm do so by addition of successive bands further and further away into the host sand until they are considered as separate structures entirely.

The different field observations show an evidence for a chronology in the development of isolated CDBs, CDB clusters and slip surfaces or narrow slip zones. Generally, the observations show that clusters are cut by the slip surfaces and narrow slip zones (Fig. 6b). The different scan-lines (Figs. 10 and 11) also show that slip surfaces and narrow ultracataclastic fault zones can exist in the middle or at the edge of clusters of CDB zones, but they never exist without clusters. On the other hand, many clusters exist with no associated slip surface or narrow ultracataclastic zone. These observations suggest that the clusters of CDB zones formed first, some of which then went on to localise the deformation by

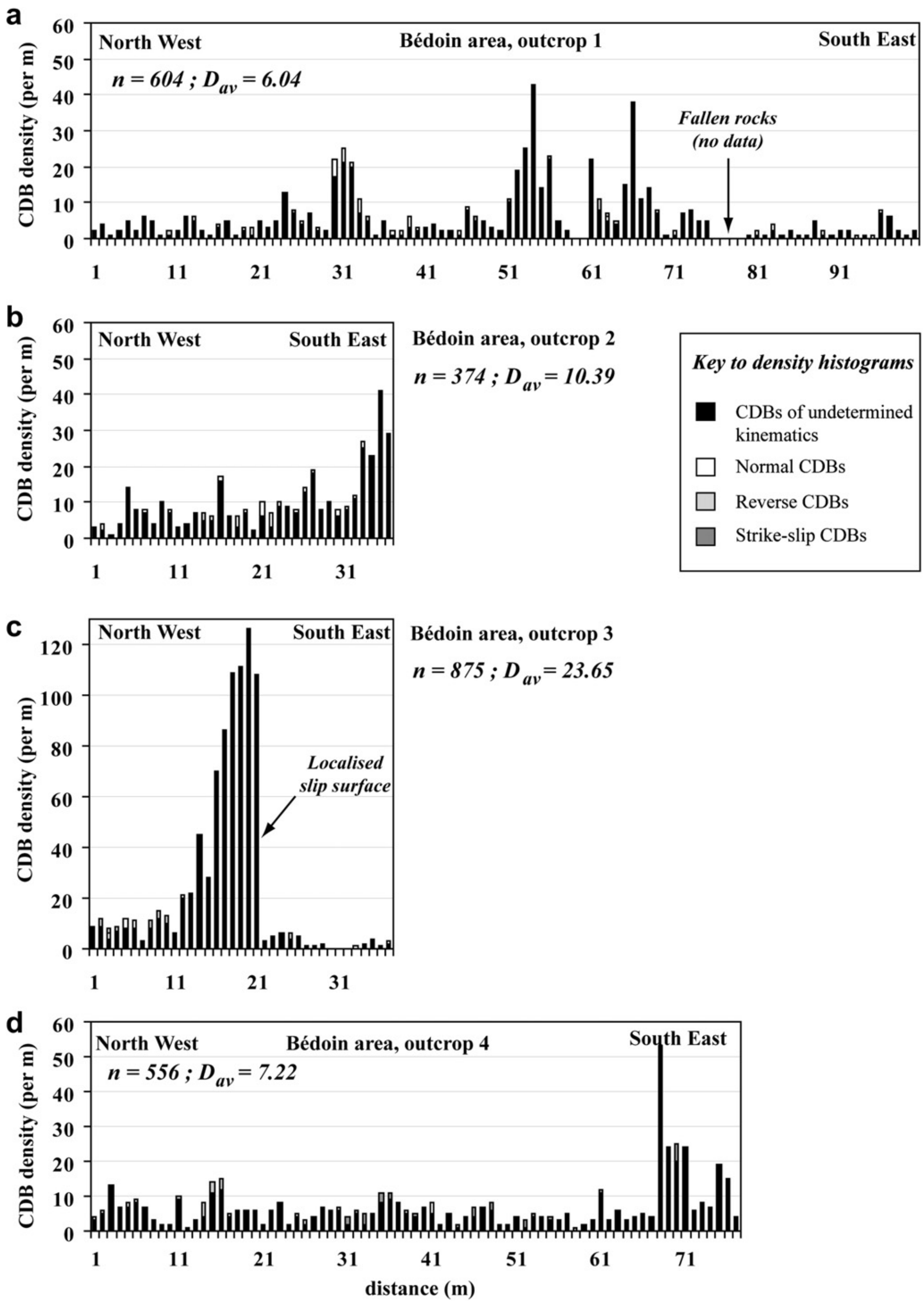

Fig. 11. Graph of CDB densities for the reverse, normal and strike-slip structures recorded along scan-lines with a total length of 250 m in the "*Le Cros*" quarry in the Bédoin area. Density is defined as the number of CDBs per square metre. As for the Massif d'Uchaux case, the CDB density overall is moderate but variable, with localisation of deformation within clusters of deformation bands. For each outcrop, *n* is the total number of deformed structures and D_{av} is the mean average density.

generation of discrete slip planes or narrow slip zones of highly deformed ultracataclasite.

5. Discussion

Spatial distributions and geometric properties of CDBs and larger faults were measured in three different areas of the *Bassin du Sud-Est* along scan-lines of totalling 717 m in length. Systematic recording of the deformation structures has allowed us to better understand the mechanisms which control the distribution of deformation and fault growth in high-porosity sandstones.

5.1. Development of individual CDBs

The systematic recording of the deformation features along the different outcrops allow us to characterise the deformation in the high-porosity sands and sandstones and to propose a conceptual model for CDB growth (Fig. 15). First, our results show a predominance

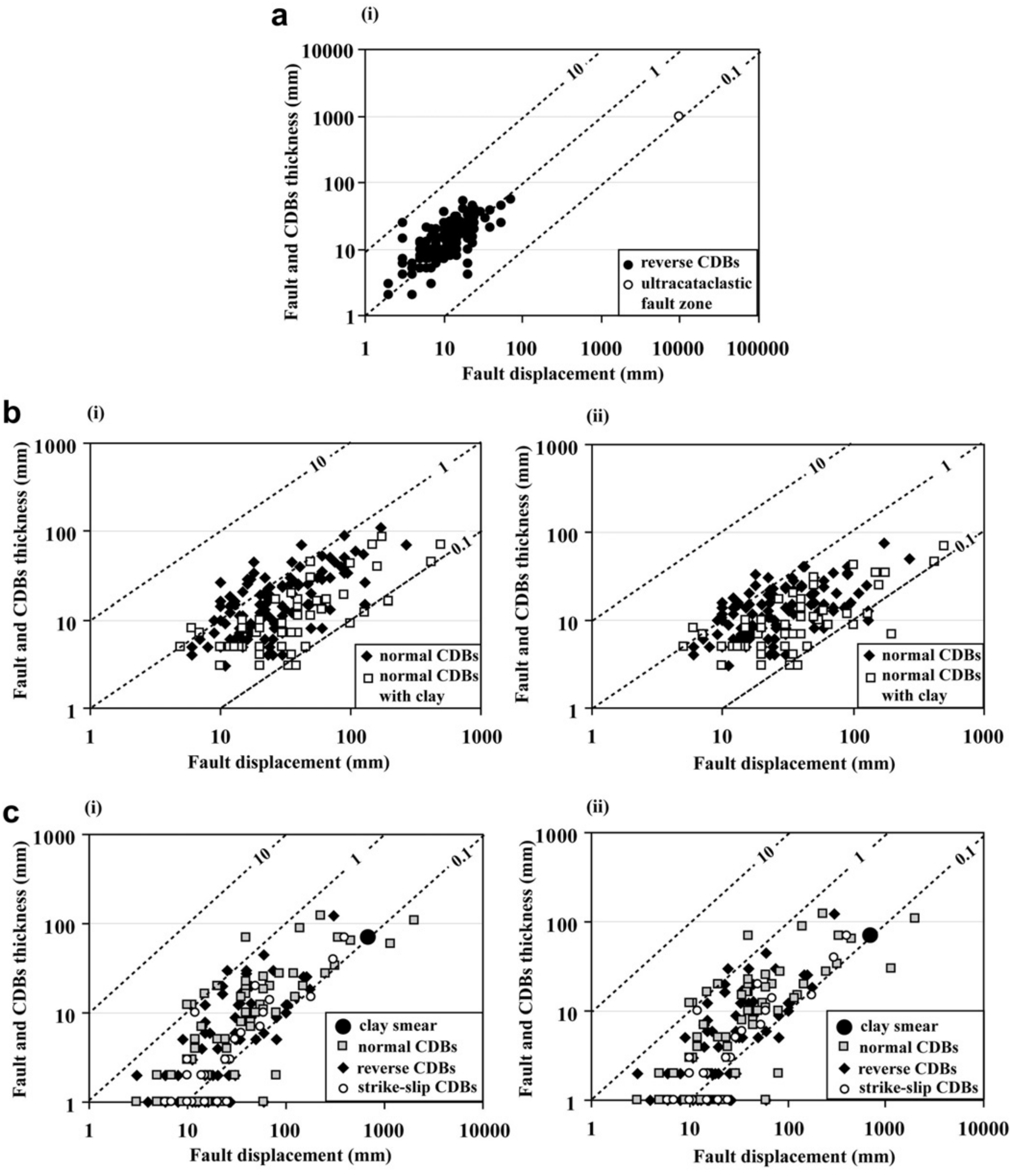

Fig. 12. Thickness–displacement relationships for CDBs, CDB zones and larger faults in the high-porosity Cretaceous sands and sandstones of Provence. (a) Data from the Orange area; (b) data from the Massif d'Uchaux area; (c) data from the Bédoin area. Data from the Massif d'Uchaux and Bédoin areas have been recorded based on two different measurement methods: (i) thickness defined as the distance between the outside edges of the outermost strands (method 1); (ii) thickness defined as the sum of individual strand thickness (method 2). The cohesion of the host rock seems to have a very important role in the thickness–displacement relationships (difference of one order of magnitude between sands and sandstones), and hence on the micro-mechanisms of deformation.

of thinner CDB zones, with 80% of all CDB zones having a thickness less than around a centimetre, as discussed in the preceding section (Fig. 13). The frequency distribution of thickness/displacement, skewed towards the narrower structures, is significant in considering fault growth. The thinner features grow during continued displacement with a proportional increase in thickness up to around 5 cm, by an increase of the number of individual bands which constitute a CDB zone (Stages 1 and 2 in Fig. 15a and b). Additional bands become spaced further and further away from the CDB zone, so that beyond around 100 mm thickness, later strands are far enough away to be counted as separate structures (see definition in the section on data acquisition). Nevertheless, the field data presented (Figs. 12 and 14) suggest an upper limit of CDB zone thickness of around 0.1–0.2 m, beyond which deformation jumps to a new band entirely.

There is, on average, a difference in the thickness–displacement ratio between the smaller CDB zones and the larger faults, for all those structures with displacements above around 0.5 m. This difference is clearest for the data from Orange (Fig. 12a). For the smaller features ($d < 200$ mm), there is a proportional increase in thickness with displacement, albeit with a scatter in thickness–displacement ratios between 0.1 and 2. The larger structures ($d > 0.5$ m) show thickness-to-displacement ratios less than 0.2, i.e. at or below the thickness–displacement ratio range of the smaller-displacement structures (Fig. 12), suggesting that the growth process does not operate as efficiently at larger displacements. Indeed, the development of ultracataclastic fault rock textures in the larger-displacement structures gives the impression of even more localised deformation. Studies show that ultracataclastic fault core zones in high-porosity sandstones elsewhere also have much narrower thickness-to-displacement ratios than associated CDBs (e.g. Shipton et al., 2005). Where clay is involved, thickness–displacement faulted clay values have, on average, lower ratios than the structures without clay, demonstrating that the

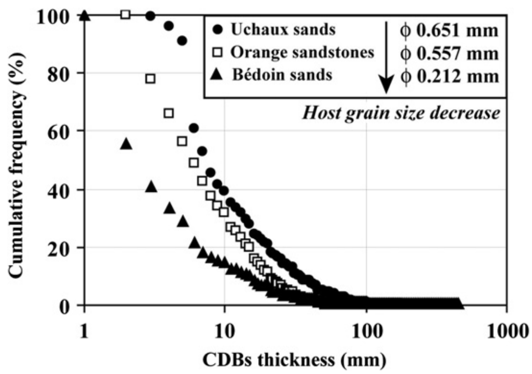

Fig. 13. Frequency distribution of CDB zone and fault zone thicknesses for cataclastic deformation bands and larger faults in the three different study areas of Provence. The thickness is defined as the distance between the outside edges of the outermost bands (method 1). The average grain size of the host rock is given for each outcrop by the symbol ϕ.

incorporation of even small amounts of clay into the deformation bands may preferentially localise deformation or at least partially inhibit wall rock wear and deformation band widening.

The observation that CDB zones grow by the addition of new peripheral bands instead of continued deformation on the existing ones may, at first sight, be taken as evidence of work hardening (e.g. Underhill and Woodcock, 1987). Nevertheless, stress perturbations around the CDB zone which encourage localisation of the new bands adjacent to the CDB zone, coupled with intragranular microcracking around the CDB zone as it develops (Wibberley et al., 2007), suggest that other factors may also play a role, particularly as laboratory experiments do not show a strength increase of samples as individual strands form in a developing CDB zone (Mair et al., 2000). The data corresponding to the larger CDB zones (with a thickness more than ~10 cm) show a diminishing thickness growth as displacement progressively increases, by a decreasing role played by the addition of new bands to the CDB zone structure. Thus the data from the different sand and sandstone outcrops show two different growth mechanisms, which are scale dependent. The thinner CDB zones grow by systematic addition of new bands, according to a work-hardening process and/or by stress perturbations encouraging adjacent intragranular fracturing. For CDB zones wider than around 10 cm however, the data suggest that these work hardening and/or other processes cease to dominate. The reason for such a transition may be one or more of the following possibilities:

1. The larger CDB zones are typically longer – their development may be limited by bed thickness and mechanical properties of adjacent beds (e.g. Schultz and Fossen, 2002) as predicted by numerical modelling of instability development during multilayer deformation (e.g. Schueller et al., 2005). However, beds are often thicker than the height of the outcrop (e.g. several metres to several tens of metres), making this difficult to assess.
2. Stress perturbations may vary with CDB zone thickness, length and displacement gradient. It is possible that wider, longer CDB zones will have wider zones of stress perturbation, so additional bands could be generated further and further away from the original CDB zone to the point where they are no longer recorded as part of the same single ("multistrand") CDB zone.
3. Grain size and grain point contact geometry could be controlling factors (e.g. Cundall, 1989), particularly given that smaller average host sand grain size seems to cause narrower CDBs (Fig. 13).

5.2. Development of CDB networks

The three study areas show deformation patterns which can be related to one or more different tectonic events. For the sandstones from the Orange area, the structures are mostly conjugate reverse CDB faults corresponding to Pyrenean–Provençal shortening. Here, only a few later, normal faults are present, related to Oligocene–Miocene extension. Evidence of deformation structures corresponding essentially to one single tectonic event at this outcrop is highly significant in terms of allowing us to make interpretations of how this network of structures developed during the single tectonic event. In terms of the spatial distribution of the CDBs documented from the scan-line data (Fig. 8), two main interpretations can be made:

1. Firstly, the distribution of the deformation along the outcrop is relatively homogeneous with a moderately high density of CDBs and an addition of high density of deformation which corresponds to a localisation of the deformation in a few clusters of CDBs such as "ladder zones". Such a persistent density distribution over a transect of c. 250 m is important because it suggests an overall relatively homogeneous bulk strain (shortening) accommodated by these CDBs over a relatively large distance, in comparison to previous studies which mostly suggest CDBs are formed as clusters of CDBs around larger faults, such as damage zones developed by progressive displacement along the fault (e.g. Shipton and Cowie, 2001; Du Bernard et al., 2002b; Johansen and Fossen, 2008).
2. Secondly, there is a general inverse relationship between the undulating density of one of the conjugate sets and the density of the other (Fig. 8), with alternating density peaks and troughs of one set mirroring the troughs and peaks of the conjugate set. The sum of the two conjugate distributions is a much more continuous deformation distribution than the clustered tendency of each of the two conjugate sets individually (Fig. 9). These field observations allow us to suggest that deformation proceeded by development of two conjugate sets of CDBs, of opposing dips, during the same tectonic event. At the beginning of the tectonic event the deformation is accommodated by a random distribution of each conjugate set. As deformation proceeds, further generation of the CDBs of one set is inhibited in regions where earlier CDBs of the other set are already present (Fig. 15a). The areas not deformed early on in the process may experience a higher number of CDBs generated later. The result of this growth process is that regions with a high density of faults from one set have a lower density in the other, and vice-versa. This CDB growth process by competition between two opposing conjugate sets during a single tectonic event results in a broadly homogeneous total (albeit undulating) deformation distribution along the outcrop.

Previous studies have suggested that deformation bands form by work-hardening processes (e.g. Aydin and Johnson, 1983; Underhill and Woodcock, 1987). Furthermore, work-hardening processes at fault tips and relay zones have been evidenced by the generation of ladder zones between segment tips (e.g. Schultz and Balasko, 2003; Okubo and Schultz, 2005, 2006). However, our field observations show that the work-hardening nature inferred for CDB generation may influence the population at the network scale as well as at the scale of the fault tip, thus causing an increase in the mechanical strength of the rock mass as well as the individual deformation band structure. Hence, it is easier for a conjugate set to develop in a region with low density of earlier deformation structures. Although overall the two sets are generally synchronous, as shown by the mutual cross-cutting relationships in different places

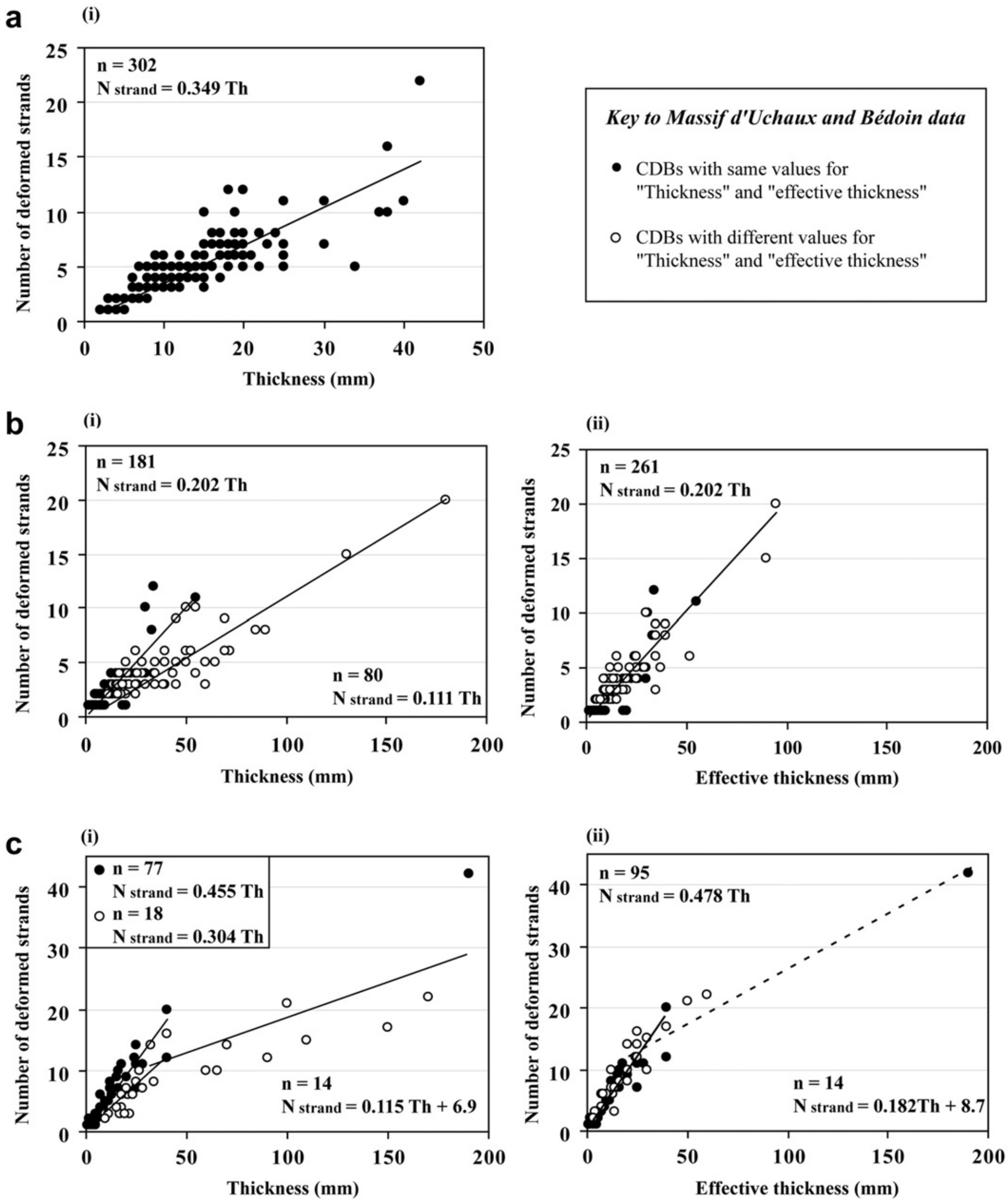

Fig. 14. Relationship between number of bands and thickness for CDB zones and larger faults in the high-porosity Cretaceous sands and sandstones of Provence. (a) Data from the Orange area; (b) data from the Massif d'Uchaux area; (c) data from the Bédoin area. Data from the Massif d'Uchaux and Bédoin areas have been recorded based on two different measurement methods: (i) thickness defined as the distance between the outside edges of the outermost bands (method 1); (ii) thickness defined as the sum of individual band thickness (method 2). The linear regressions presented on these graphs are the lines of best-fit, most of which are constrained to pass through the origin; the equations are given for each one. For the graphs (c), the second linear regression corresponds to the lines of best-fit of the largest structures, which are not constrained to pass through the origin. The regression in (c ii) is given as a dotted line because of the small number of these structures.

(Fig. 5), the preferential development of one set in a certain region probably depends on it arriving in that region by chance before the other set. Despite this seeming randomness, it is nevertheless possible that the spacing of peaks and troughs in the densities of each conjugate set, in this case around 60 m along the scan-line, so around 30 m perpendicular to any one set, is related to mechanical unit thickness, although the base of the unit is below ground level so we can not assess this.

It was not possible to test this model for conjugate CDB development on the other study areas because they have recorded deformation from two or three superimposed tectonic events, and in many cases it is not possible to attribute an individual CDB to a particular tectonic event. Because of this, the statistical clustering analysis performed on the Orange data (Section 3.2.1) was not performed on the other data sets as it would not have been meaningful. However, all the Massif d'Uchaux outcrops expressed similar patterns. For each outcrop there is a generally moderate density of deformation structures with the addition of clusters of CDB zones which localised the deformation (Fig. 10). The same deformation patterns exist also in the outcrops from the incohesive sands of the Bédoin area (Fig. 11). In these cases, the majority of the CDBs are normal-sense structures generated during extension. It therefore seems likely that the difference in clustering tendency between these outcrops and the distributed nature of the deformation at Orange is simply due to kinematic type of deformation, with shortening encouraging further generation of CDBs throughout the volume by system hardening during compression (Fig. 15a). However, other factors such as differences in burial depth

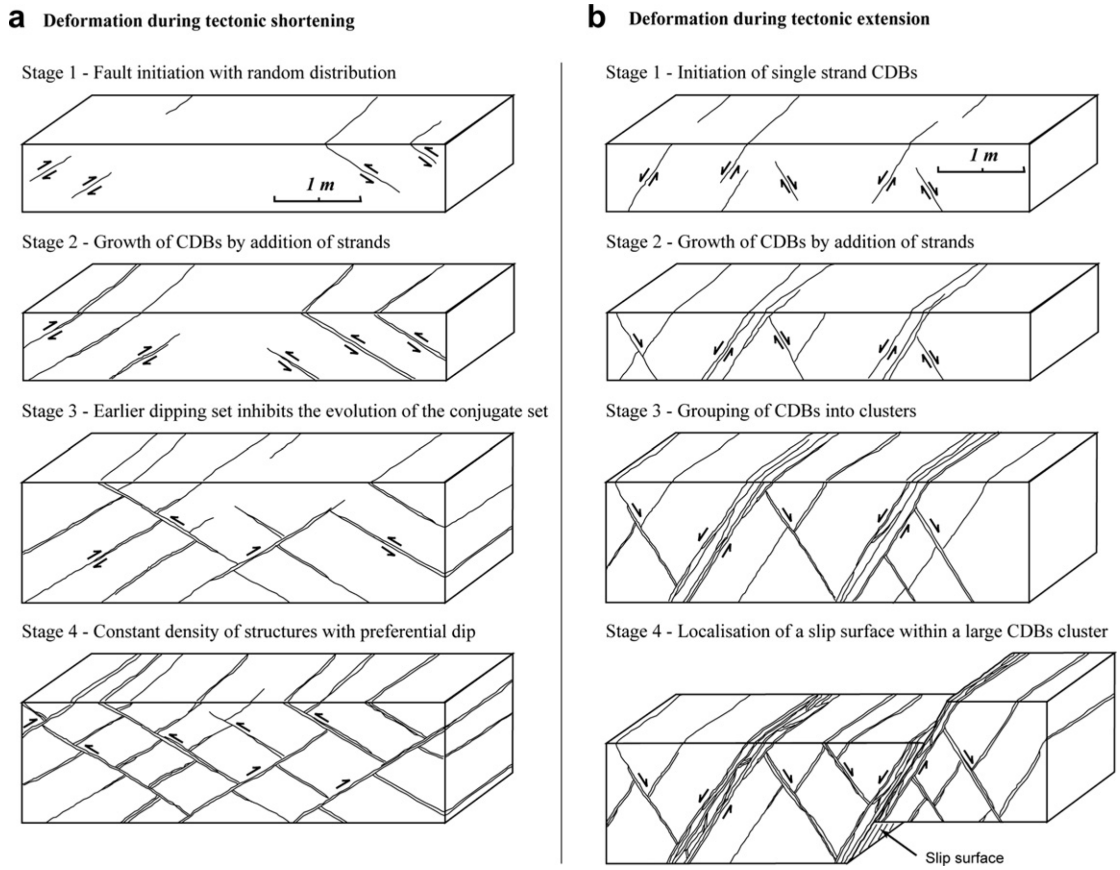

Fig. 15. Series of block diagrams showing the sequential evolution of deformation from a single band to different sets in a network, with possible localised faulting, during a single tectonic event. (a) A compressive tectonic event. (Stage 1) Random distribution of the deformation at the beginning of the tectonic event. (Stage 2) Evolution of single CDBs to larger CDB zones. (Stage 3) Further deformation results in cross-cutting of CDB zones by conjugate structures, but the previous structures inhibit further development of the conjugate set in places. (Stage 4) As deformation continues, the structural network evolves towards a broadly constant density of conjugate structures. (b) An extension tectonic event. (Stage 1) Initiation of single CDBs at the beginning of the tectonic event. (Stage 2) Evolution of single CDBs to larger CDB zones. (Stage 3) Localisation of the deformation within some clusters of CDB zones. (Stage 4) As deformation continues, a slip surface or narrow slip zone grows within a zone of deformation band clustering.

at the time of deformation, which is difficult to constrain here, may also play a role. It seems likely that differences in tectonic loading path have had an effect on the spatial distribution of the resulting deformation.

5.3. Development of higher-displacement “mature” faults and slip planes

Previous qualitative and semi-quantitative work on some of the outcrops presented here found that larger ultracataclastic fault zones and localised slip surfaces often formed where there was a high density of CDBs from a previous tectonic event (Wibberley et al., 2007). The new work expands on the previous study by the thorough collection of statistical data from scan-lines, such as spatial variations in density, as well as studying additional outcrops. It has been found that larger-displacement fault zones and localised slip surfaces can also form in the same tectonic event as the CDBs, but in this case they exist within, or at the edge of clusters of CDB zones. The precise relative chronology of CDBs and larger faults is difficult to discern at outcrop in most cases, and it is possible to suggest two different hypotheses for their genetic relationship: either (a) all the background CDBs formed first, with a relatively constant density across the outcrop, followed by localisation into the clusters; or (b) the CDBs initiated in a few places, and continued deformation allowed both further development into clusters and spreading of the deformation elsewhere to form the other individual CDBs further away from the clusters.

The fact that all larger-displacement faults occur within regions of high CDB density, but that many high-density clusters exist without larger faults, suggests that the clusters formed first, only some of which suffered continued deformation localisation and generation of ultracataclastic faults and discrete slip surfaces (Fig. 15b, stage 4). In other words, a larger fault is not a prerequisite for generating peripheral clusters of CDBs (as in a “damage zone”) in the study areas examined, but these larger faults localise on pre-existing cluster zones to accommodate further strain. In fact, in extensional contexts such as those which generated the structures studies in the Urchaux and Bédoin areas, it is much easier to form a slip zone. In the case of reverse deformation, it seems that it is much more difficult to obtain a localised slip plane or narrow slip zone — the example of deformation bands accommodating shortening at Orange never achieved a state of localisation to evolve into a large structure; deformation is likely to be transferred into a different lithological layer before such a high deviatoric stress is achieved.

The progressive localisation of deformation through time during extension, from an undulating “background” CDB density pattern and the clustering of CDBs through to formation of larger-displacement ultracataclastic fault zones and initiation of discrete slip surfaces may therefore be at least partly a function of the extensional tectonic regime and associated loading path. It is often tempting to associate such deformation localisation with material softening of the slip zones, yet in reality localisation is also controlled by other factors such as system geometric constraints

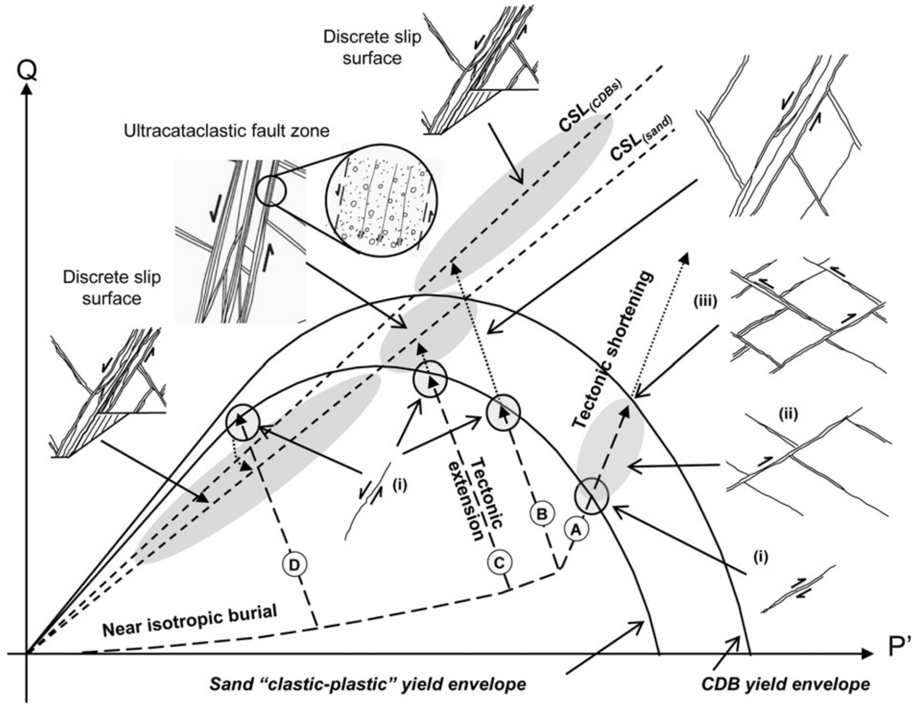

Fig. 16. A Q–P′ map of generation of deformation structures in high-porosity sand. CSL indicates Critical State Line. Four different hypothetical stress paths are indicated (labelled A–D), each producing a different range of structures. See text for details.

and is not simply a function of material softening (e.g. Hobbs et al., 1990). In the case of extension, it has been suggested that elastic unloading of the wall during normal faulting may inhibit the continued generation of new deformation bands around the fault, whilst the main fault zone continues to deform. As the faults grow up-dip and down-dip they will be controlled by other system parameters such as bed thickness and the mechanical contrast with adjacent beds, so that eventually the mechanical properties of the fault will be controlled by system constraints at a larger scale, possibly with damage zone accumulation contributing to further fault zone development.

The importance of loading path on deformation structural evolution can be illustrated by Q–P′ maps (Fig. 16). These plot the stress paths in terms of differential stress (Q) against effective mean stress (P′) as commonly done in soil mechanics. On such plots, the range of stress states at the onset of plastic deformation can be plotted (a yield envelope), as can the fields in which deformation occurs by compaction, dilation or the critical state line of constant-volume deformation between the two. Plastic yield envelopes continuously evolve as the sand is subjected to compaction and/or tectonic deformation until they reach a "clastic–plastic" yield envelope at which point cataclastic deformation bands are generated (Bolton and McDowell, 1997; Wibberley et al., 2007). For this reason, several authors have recently used a framework of soil mechanics to better understand the initiation of cataclastic deformation bands, seen as a phenomenon of plastic deformation which may be either compactant, dilatant or constant-volume (e.g. Schultz and Siddharthan, 2005; Aydin et al., 2006; Wibberley et al., 2007). Deformation accommodating much larger slip than typical deformation bands, usually by discrete slip surfaces and/or ultracataclastic fault zones, is considered to occur on the critical state line of isovolumetric deformation. Although there is no *a priori* connection between the critical state line (as a range of stress states) and localisation (as a description of deformation distribution), microstructural studies of the ultracataclastic fault zones suggest constant-volume granular flow operated during shearing, supported by classical soil mechanics experiments after a given shear strain (e.g. Mandl et al., 1977).

Fig. 16 illustrates four hypothetical loading paths on a Q–P′ map of differential stress (Q) against effective mean stress (P′), the first path (A) being tectonic compression, the other ones being different cases of extension (B–D). In all cases, cataclastic deformation bands initiate at the "clastic–plastic" yield envelope (stage i), in most cases on the right hand side ("cap" side) of the Q peak in the yield envelope, suggesting compaction. The strength of the CDB itself defines a new yield envelope, being stronger than the host sand. In the case of shortening, CDBs continue to be generated until they start to cross each other, at which point network hardening occurs and the stress path moves up towards the CDB yield envelope (stage ii on stress path A). A critical density is achieved at which the bulk stress state lies in fact on the CDB yield envelope (stage iii). Further increase in stress is required to continue deformation, but it is uncertain whether this can continue to the critical state line (Fig. 16) – it is more likely that failure of an adjacent bed will lead to a thrust fault propagating into the porous sand bed.

In extension, on the other hand, the exact sequence and type of structures generated is suggested to depend on the starting position of the effective tension loading with respect to the clastic–plastic and CDB yield envelopes. In loading path B (Fig. 16), the path continues to increase differential stress and hence generate CDBs until, like path A, a critical density is reached (network hardening). Beyond this, differential stress continues to increase until the critical state line of the (bulk) deformation band material is reached at which point faulting occurs by ultracataclasic in a zone with granular flow, and/or by forming discrete slip surfaces. Field evidence indicates that slip surfaces in this context localise within clusters of CDB zones or at the competence contrast between CDB clusters and host sand. In loading path C (Fig. 16), the critical state line for the sand is reached as the stress path continues to move through the compactant regime during network hardening before the CDB yield envelope is reached, suggesting that faulting will occur in the sand by localised ultracataclasis. Finally, in loading path D (Fig. 16), the CDB initiation occurred at greater differential stress than the critical state line (and on the dilatant side to the left of the yield envelope peak), suggesting that further deformation will quickly result in deformation localisation in the sand on discrete slip surfaces along with unloading. This softening effect may be enhanced by non-associated Coulomb plasticity softening (Mandl, 1988) as described by Wibberley et al. (2007).

6. Conclusions

The statistical analyses of the spatial distributions and geometrical properties of cataclastic deformation bands and larger ultracataclastic fault zones in Cretaceous high-porosity sands and sandstones from Provence, SouthEast France, allow us to evaluate the controls on deformation distribution and fault growth mechanisms. The main results can be summarized as follows:

1. CDB density distributions along the Orange outcrop suggest that deformation was accommodated by two conjugate sets, each of heterogeneous distribution, during the same tectonic event. In any one place, where there is a higher density of faults from the first set, there is a lower density in the second, and where there is a lower density of faults from the first set, there is a higher density in the second. The result of this fault growth process is a broadly homogeneous total deformation along the outcrops which developed by a system-hardening mechanism during shortening. The frequency of the density undulations of each of the two conjugate sets may be related to mechanical bed thickness.
2. The Massif d'Uchaux and Bédoin outcrops have moderate, undulating densities of mainly normal-sense CDBs associated with extension. Some zones are present with anomalously high CDB densities, where CDB zones are organized into clusters, some of which contain larger-displacement ultracataclastic fault zones or discrete slip surfaces. This distribution differs from the reverse-sense CDBs at Orange. Thus for the first deformation event to strongly affect the outcrop, the clustering tendency is dependant on kinematics and therefore tectonic loading path. Thickness growth of CDB zones, however, is independent of these, but dependent on host grain size with thicker CDB zones forming in coarser sand/sandstone.
3. CDB zones grow by a proportional increase of thickness with displacement due to the addition of new individual bands within the zone, corresponding to a work-hardening process at the scale of the zone. As thickness achieves a certain value on the order of ~ 10 cm, the generation of additional bands does not continue in proportion to thickness growth. In these larger CDB zones, the new outer bands are generated further and further into the host sand away from the zone. Hardening processes cease to dominate for these larger CDB zones, and further deformation occurs with clustering of CDB zones followed in some cases by generation of the larger-displacement ultracataclastic faults and discrete slip surfaces which grow with increasing localisation of deformation.

Acknowledgements

The first author was supported by a doctorate student MRT stipend from the French Ministry for Higher Education and Research. Access to the active quarries was granted by the operating company SIFRACO who is gratefully acknowledged. Thorough reviews by Geoffrey Rawling and Richard Schultz helped clarify much of the text, and we are also grateful to Zoe Shipton for editorial guidance.

References

Antonelini, M., Aydin, A., 1994. Effect of faulting on fluid flow in porous sandstones: petrophysical properties. American Association of Petroleum Geologists Bulletin 78, 335–377.
Antonelini, M., Aydin, A., 1995. The effect of faulting on fluid flow in porous sandstones: geometry and spatial distribution. American Association of Petroleum Geologists Bulletin 79, 642–671.
Antonellini, M.A.A., Aydin, A., Pollard, D.D., 1994. Microstructure of deformation bands in porous sandstones at Arches National Park, Utah. Journal of Structural Geology 16, 941–959.
Aydin, A., 1978. Small faults formed as deformation bands in sandstones. Pure and Applied Geophysics 116, 913–930.
Aydin, A., Johnson, D., 1978. Development of faults as zones of deformation bands and as slip surfaces in sandstone. Pure and Applied Geophysics 116, 931–942.
Aydin, A., Johnson, D., 1983. Analysis of faulting in porous sandstones. Journal of Structural Geology 5, 19–31.
Aydin, A., Borja, R.I., Eichhubl, P., 2006. Geological and mathematical framework for failure modes in granular rock. Journal of Structural Geology 28, 83–98.
Bolton, M.D., McDowell, G.R., 1997. Clastic mechanics. In: Fleck, N.A., Cocks, A.C.F. (Eds.), IUTAM Symposium on Mechanics of Granular and Porous Materials. Kluwer, Dordrecht, pp. 35–46.
Cundall, P.A., 1989. Numerical experiments on localization in frictional materials. Ingenieur-Archiv 59, 148–159.
Davis, G.H., 1999. Structural geology of the Colorado Plateau regional of southern Utah, with special emphasis on deformation bands. Geological Society of America Special Paper 342.
Debrand-Passard, S., Courbouleix, S., Lienhardt, M.J., 1984. Synthèse géologique du Sud-Est de la France. Mémoire du Bureau de Recherches Geologiques et Minières, (BRGM), 125, Orleans, France.
Delfaud, J., Dubois, P., 1984. Le basin du Sud-Est. In: Gubler, Y. (Ed.), Dynamique des bassins sédimentaires. Livre jubilaire BRGM, Orleans, France.
Du Bernard, X., Eichhbul, P., Aydin, A., 2002a. Dilation bands: a new form of localized failure in granular media. Geophysical Research Letters 29, 2176. doi:10.1029/2002GL015966.
Du Bernard, X., Labaume, P., Darcel, C., Davy, P., Bour, O., 2002b. Cataclastic slip band distribution in normal fault damage zones, Nubian sandstones, Suez rift. Journal of Geophysical Research 107, 103–114.
Evans, J.P., 1990. Thickness–displacement relationships for fault zones. Journal of Structural Geology 12, 1061–1065.
Fossen, H., Odinsen, T., Færseth, R.B., Gabrielsen, R.H., 2000. Detachments and low-angle faults in the northern North Sea rift system. In: Nøttvedt, A. (Ed.), Dynamics of the Norwegian margins. Special Publications, Geological Society, London, vol. 167, pp. 105–131.
Fossen, H., Schultz, R.A., Shipton, Z.K., Mair, K., 2007. Deformation bands in sandstone: a review. Journal of the Geological Society of London 164, 755–769.
Fowles, J., Burley, S., 1994. Textural and permeability characteristics of faulted, high porosity sandstones. Marine and Petroleum Geology 11, 608–623.
Gallagher Jr., J.J., Friedman, M., Handin, J., Sowers, G.M., 1974. Experimental studies relating to microfracture in sandstone. Tectonophysics 21, 203–247.
Hobbs, B.E., Mühlhaus, H.-B., Ord, A., 1990. Instability, softening and localization of deformation. In: Knipe, R.J., Rutter, E.H. (Eds.), Deformation Mechanisms, Rheology and Tectonics. Geological Society Special Publications, vol. 54, pp. 143–165.
Hull, J., 1988. Thickness–displacement relationships for fault zones. Journal of Structural Geology 10, 431–435.
Jamison, W.R., Stearns, D.W., 1982. Tectonic deformation of Wingate Sandstone, Colorado National Monument. American Association of Petroleum Geologists Bulletin 66, 2584–2608.
Johansen, T.E.S., Fossen, H., 2008. Internal geometry of fault damage zones in interbedded siliclastic sediments. In: Wibberley, C.A.J., Kurz, W., Imber, J., Holdsworth, R.E., Collettini, C. (Eds.), The Internal Structure of Fault Zones: Implications for Mechanical and Fluid-Flow Properties. Geological Society Special Publication, vol. 299, pp. 34–55.
Mair, K., Main, I., Elphick, S., 2000. Sequential growth of deformation bands in the laboratory. Journal of Structural Geology 22, 25–42.
Mandl, G., 1988. Mechanics and Tectonics of Faulting: Models and Basic Concepts. Elsevier, Amsterdam.
Mandl, G., de Jong, L.N.J., Maltha, A., 1977. Shear zones in granular material. Rock Mechanics 9, 95–144.
Manzocchi, T., Ringrose, P.S., Underhill, J.R., 1998. Flow through fault systems in high-porosity sandstones. In: Coward, M.P., Daltaban, T.S., Johnson, H. (Eds.), Structural Geology in Reservoir Characterisation. Geological Society, London, Special Publications, vol. 127, pp. 65–82.
Matthäi, S.K., Aydin, A., Pollard, D.D., Roberts, S.G., 1998. Numerical simulation of departures from radial drawn in faulted sandstone reservoirs with joints and deformation bands. In: Jones, G., Fisher, Q., Knipe, R.J. (Eds.), Faulting, Fault

Sealing and Fluid Flow in Hydrocarbon Reservoirs. Geological Society, London, Special Publications, vol. 147, pp. 157–192.
Okubo, C.H., Schultz, R.A., 2005. Evolution of damage zone geometry and intensity in porous sandstone: insight gained from strain energy density. Journal of the Geological Society of London 162, 939–950.
Okubo, C.H., Schultz, R.A., 2006. Near-tip stress rotation and the development of deformation band stepover geometries in mode II. Geological Society of America Bulletin 118, 343–348.
Priest, S.D., Hudson, J.A., 1981. Estimation of discontinuity spacing and tracing length using scanline survey. International Journal of Rock Mechanics and Mining Sciences and Geomechanics Abstracts 18, 183–197.
Robertson, E.C., 1983. Relationship of fault displacement to gouge and breccia thickness. Mining Engineering 35, 1426–1432.
Saillet, E., 2009. La localisation de la déformation dans les grès poreux: caractérisation d'un analogue de réservoir faillé dans le Bassin du Sud-Est, Provence, France. Doctorate thesis, University of Nice-Sophia Antipolis, France, 273 p.
Shipton, Z.K., Cowie, P.A., 2001. Damage zone and slip-surface evolution over μm to km scales in high-porosity Navajo sandstone, Utah. Journal of Structural Geology 23, 1825–1844.
Shipton, Z.K., Evans, J.P., Thompson, L.B., 2005. The geometry and thickness of deformation-band fault core and its influence on sealing characteristics of deformation-band fault zones. In: Sorkhabi, R., Tsuji, Y. (Eds.), Faults, Fluid Flow and Petroleum Traps. American Association of Petroleum Geologists Memoir, vol. 85, pp. 181–195.
Scholz, C.H., 1987. Wear and gouge formation in brittle faulting. Geology 15, 493–495.
Schultz, R.A., Fossen, H., 2002. Displacement–length scaling in three dimensions: the importance of aspect ratio and application to deformation bands. Journal of Structural Geology 24, 1389–1411.
Schultz, R.A., Balasko, C.M., 2003. Growth of deformation bands into echelon and ladder geometries. Geophysical Research Letters 30, 2033. doi:10.1029/2003GL018449.
Schultz, R.A., Siddharthan, R., 2005. A general framework for the occurrence and faulting of deformation bands in porous granular rocks. Tectonophysics 411, 1–18.
Schueller, S., Gueydan, F., Davy, P., 2005. Brittle–ductile coupling: role of ductile viscosity on brittle fracturing. Geophysical Research Letters 32, L10308. doi:10.1029/2004GL022272.
Torabi, A., Braathen, A., Cuisiat, F., Fossen, H., 2007. Shear zones in porous sand: insights from ring-shear experiments and naturally deformed sandstones. Tectonophysics 437, 37–50.
Underhill, J.R., Woodcock, N.H., 1987. Faulting mechanisms in high porosity sandstones; New Red Sandstone, Arran, Scotland. In: Jones, M.E., Preston, R.M.F. (Eds.), Deformation of Sediments and Sedimentary Rocks. Geological Society, London, Special Publications, vol. 29, pp. 91–105.
Wibberley, C.A.J., Petit, J.P., Rives, T., 2000. Mechanics of cataclastic 'deformation band' faulting in high-porosity sandstone, Provence. Comptes Rendus de l'Academie des Sciences, Paris 331, 419–425.
Wibberley, C.A.J., Petit, J.P., Rives, T., 2007. The mechanics of fault distribution and localization in high-porosity sands, Provence, France. In: Lewis, H., Couples, G.D. (Eds.), The Relationship between Damage and Localisation. Geological Society, London, Special Publication, vol. 289, pp. 19–46.
Wibberley, C.A.J., Yielding, G., DiToro, G., 2008. Recent advances in the understanding of fault zone internal structure: a review. In: Wibberley, C.A.J., Kurz, W., Imber, J., Holdsworth, R.E., Collettini, C. (Eds.), The Internal Structure of Fault Zones: Implications for Mechanical and Fluid-Flow Properties. Geological Society Special Publication, vol. 299, pp. 5–33.
Wong, T.-F., David, C., Zhu, W., 1997. The transition from brittle faulting to cataclastic flow in porous sandstones: mechanical deformation. Journal of Geophysical Research 102, 3009–3025.